

MICROSTRIP - FED SLOT ARRAY

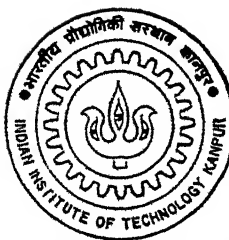
by

PRADEEP KUMAR PALIWAL

TH
EE/1996/M

P176m

1996



DEPARTMENT OF ELECTRICAL ENGINEERING

INDIAN INSTITUTE OF TECHNOLOGY KANPUR

March, 1996

MICROSTRIP-FED SLOT ARRAY

A Thesis Submitted
in Partial Fulfillment of the Requirements
for the Degree of
Master of Technology

by

Pradeep Kumar Paliwal

to the

DEPARTMENT OF ELECTRICAL ENGINEERING
INDIAN INSTITUTE OF TECHNOLOGY, KANPUR

March 1996

11 100-708 /EE

EE-1996-M-PAL-MIC

ISS. NO. A. 121278



Certificate

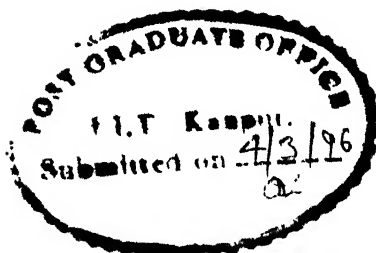
It is certified that the work contained in the thesis entitled "**MICROSTRIP-FED SLOT ARRAY**", by **Pradeep Kumar Paliwal**, has been carried out under my supervision and that this work has not been submitted elsewhere for a degree.

March 1996

M.Sachidananda 43196
Dr. M Sachidananda

Professor

Department of Electrical Engineering
I.I.T. Kanpur



ACKNOWLEDGEMENT

I wish to record my sincere gratitude to my guide Prof. M. Sachidananda for his kind supervision, constant guidance, encouragement and helpful advice throughout the course of this study.

I am deeply indebted to my colleagues Harish, Apusivdas and Arun Sehgal for the successful completion of this work. I express my thanks to Dr. A. Biswas who always encouraged me. I also like to thank Shri Chaitanyababu and Rajeev for cooperation.

I am grateful to my department and D.T.S.R. for having provided me the opportunity to work towards my M.Tech. degree at I.I.T. Kanpur.

I take this opportunity to thank all my friends who have directly or indirectly contributed towards the successful completion of this work.

I acknowledge the technical help rendered by Shri P.H. Tewari and Ram Bahadur of A.C.E.S. Workshop and Shri Dinesh Kumar and S.K. Kole of P.C.B. Lab.

My wife, Renu and daughters, Swati, Shubhra deserve a word of special priase for the sacrifices they have made, for the sake of my knowledge seeking persuit.

P.K. PALIWAL

ABSTRACT

In the last few years, rural radio network has been one of the major concepts that is being implemented in India, to take telecommunication to remote areas where laying of telephone line is not factual, in terms of cost and maintenance. Rural radio uses a central base station and several sub-station which communicate to the central base station. Each sub-station is connected to several subscribers via local telephone network. The base station needs an antenna with a nominal gain and omnidirectional coverage so that it can communicate with any of the sub-station in the region. The work is an attempt to design such a base station antenna at 3.2 GHz with a bandwidth of about 200 MHz.

The design approach has been entirely experimental. After a survey of the feasible configuration for the base station antenna, a microstrip-fed slot array was selected. A set of three such arrays arranged around a circle to obtain omnidirectional coverage. One such linear array is designed, fabricated and tested in the laboratory. This thesis is the study of this development effort.

One of the major constraints in this work was the availability of the microwave substrate and the cost involved in importing the substrate. For building an efficient antenna, low loss microwave substrate is a must. However, to demonstrate the concept and prove the feasibility, we studied a locally available

glass epoxy substrate which has a much high loss factor. The major effect of the lossy substrate would be a reduction in the overall gain of the antenna but would not affect the pattern characteristics. Based on the requirements of a base station antenna, the specification for the antenna were worked out first and then the configuration was arrived at. Once the array configuration was decided upon, the design involved fabricating a single slot radiator and characterization. Evaluation of mutual coupling among the array elements, design of corporate feed network in microstrip form and then integration of the complete array.

To make the slot radiation unidirectional, a reflector plate was introduced on one side. The slot dimensions and reflector plate spacings were optimised for best performance of individual slot radiator. Then for this slot configuration, mutual coupling was experimentally evaluated by fabricating three slots on one substrate with appropriate feed network. From the measured data on a single slot and mutual coupling, array feed network was designed on microstrip.

The complete linear array with reflector plate was fabricated and tested in the laboratory for input VSWR and the pattern. Measured array directivity was about 15 dB at 3.2 GHz, with 120° 5 dB beamwidth in the horizontal plane and 3 dB beamwidth is at about 100° . The input minimum return loss in the band from 3.1 to 3.3 GHz was -7.0 dB. At the center frequency it is -11.0 dB. However, the measured gain was much less than the required gain

because of the lossy substrate. This work only demonstrates the feasibility of the concept and for actual usable antenna one needs to use the microwave substrate in place of glass epoxy substrate, to achieve the required gain.

CONTENTS

CHAPTER 1 : INTRODUCTION

1.1	Introduction	1
1.2	Survey of literature on omni/sector-beam antennas	2
1.3	Multi-Beam Array	4
1.4	Waveguide Slot Array	4
1.5	Configuration of Slot Array Chosen	6
1.6	Contents of The Thesis	8

CHAPTER 2 : EXPERIMENTAL STUDY OF MICROSTRIP-FED SLOT

2.1	Introduction	9
2.2	Slot Geometry	11
2.3	Slot Characteristics	11
2.4	Approximate Design	17
2.5	Modification	23
2.6	Final Configuration	25
2.7	Conclusion	29

CHAPTER 3 : MUTUAL COUPLING EVALUATION

3.1	Introduction	32
3.2	Mutual Coupling Measurement Set-Up	33
3.2.1	Measured Results	33
3.3	Dipole/Slot Formulation	39
3.4	Final Mutual Coupling Model	42
3.5	Conclusion	47

CHAPTER 4 : ARRAY DESIGN

4.1	Array Specification	49
4.2	Array Factor Design	49
4.3	Design Coefficients	50
4.4	Active Impedance Computation for the Array	50
4.5	Matching/Feed Network Design	52
4.6	Fabrication and Testing	54
4.7	Results	59
4.8	Conclusion	59

CHAPTER 5 : CONCLUSIONS

5.1	Summary and Conclusions	65
5.2	Scope for Further Work	67

REFERENCES69

LIST OF FIGURES

Fig. 1.1 : Configuration of the sector-beam base-station antenna	3
Fig. 1.2 : Configuration of the 180° sector-beam array antenna	3
Fig. 1.3 : Configuration of the multi-beam base-station antenna	5
Fig. 1.4 : Slotted-waveguide linear array antenna for 50 GHz band	5
Fig. 1.5 : Three faced array configuration	7
Fig. 2.1 : Configuration of microstrip-fed slot antenna	12
Fig. 2.2 : The equivalent circuit of a slot in the ground plane of a microstrip line	12
Fig. 2.3 : Normalized equivalent impedance of the cavity backed slot versus offset of the feedline	14
Fig. 2.4 : The normalized resonant resistance versus normalized offset of a microstrip-fed slot antenna	15
Fig. 2.5 : Input impedance versus frequency of microstrip-fed slot antenna (without reflector)	19
Fig. 2.6 : Input impedance versus frequency of microstrip-fed slot antenna ($d = 36.8$ mm)	19
Fig. 2.7 : Input impedance versus frequency of microstrip-fed slot antenna ($d = 32.0$ mm)	20
Fig. 2.8 : Input impedance versus frequency of microstrip-fed slot antenna ($d = 27.2$ mm)	20

Fig. 2.9 : Input impedance versus frequency of microstrip-fed slot antenna (d = 23.4 mm)	21
Fig.2.10 : Input impedance versus frequency of microstrip-fed slot antenna (d = 19.2 mm)	21
Fig.2.11 : Input impedance versus frequency of microstrip-fed slot antenna (d = 16.0 mm)	22
Fig.2.12 : Input impedance versus slot-to-reflector spacing at 3.2 GHz	22
Fig.2.13 : Input impedance versus frequency of microstrip-fed slot antenna (without reflector)	24
Fig.2.14 : Input impedance versus frequency of microstrip-fed slot antenna (d = 20.0 mm)	24
Fig.2.15 : The magnitude of S_{11} of microstrip-fed slot antenna	28
Fig.2.16 : Input impedance versus frequency of microstrip-fed slot antenna	28
Fig.2.17 : E-plane radiation pattern of final element (reflector on strip side)	30
Fig.2.18 : H-plane radiation pattern of final element (reflector on strip side)	30
Fig.2.19 : E-plane radiation pattern of final element (reflector on slot side)	31
Fig.2.20 : H-plane radiation pattern of final element (reflector on slot side)	31
Fig. 3.1 : Configuration of three microstrip-fed slots	34
Fig. 3.2 : The magnitude of S_{11} versus frequency	35

Fig. 3.3 : The phase of S_{11} versus frequency	35
Fig. 3.4 : The magnitude of S_{12} versus frequency between two microstrip-fed slots	37
Fig. 3.5 : The phase of S_{12} versus frequency between two microstrip-fed slots	37
Fig. 3.6 : The magnitude of S_{13} versus frequency between microstrip-fed slots	38
Fig. 3.7 : The phase of S_{13} versus frequency between microstripfed slots	38
Fig. 3.8 : The magnitude of measured mutual admittance of microstrip-fed slots as a function of spacing	40
Fig. 3.9 : The phase variation of measured mutual admittance of microstrip-fed slots as a function of spacing	40
Fig.3.10 : The magnitude variation of mutual admittances of offset fed ($t = 0.123\lambda_0$) collinear complementary slots in free space, as a function of element spacing	43
Fig.3.11 : Variation of mutual admittance (half of magnitude) versus spacing of a offset fed complementary slot ($L = 0.625\lambda_0$) in free space	45
Fig.3.12 : Phase variation of mutual admittance vs. spacing of a offset fed complementary slot ($L=0.625\lambda_0$) in free space	45
Fig.3.13 : Variation of mutual admittance (half of magnitude) as a function of spacing in free space and with reflector	46

Fig.3.14 : Phase variation of mutual admittance as a function of spacing in free space and with reflector	46
Fig.3.15 : Magnitude variation of mutual admittance as a function of spacing, of microstrip-fed slots with reflector	48
Fig.3.16 : Phase variation of mutual admittance as a function of spacing of microstrip-fed slots with reflector	48
Fig. 4.1 : Design of feed network for First and Second slot	53
Fig. 4.2 : Configuration of microstrip-fed slot array. Part 'A'	55
Fig. 4.3 : Configuration of microstrip-fed slot array. Part 'B'	56
Fig. 4.4 : Configuration of eight-element microstrip-fed slot array	57
Fig. 4.5 : Magnitude of S_{11} versus frequency of microstrip-fed slot array	60
Fig. 4.6 : Theoretical pattern of the array computed by LAARAN	61
Fig. 4.7 : Excitation coefficient distribution of array versus element number computer by LAARAN	61
Fig. 4.8 : E-plane radiation pattern of microstrip-fed slot array of eight elements	62
Fig. 4.9 : H-plane radiation pattern of microstrip-fed slot array of eight elements	63

CHAPTER 1

INTRODUCTION

1.1 INTRODUCTION

Now-a-days rural radio networks are growing all over India. Rural radio network uses a central base station and several substations which communicates to the central base station. These substations are connected to several subscribers via local telephone network. This type of network is economically viable, specially in hilly and remote areas where the population density is low. The base station of this type of network requires omnidirectional and high gain antenna. Various types of base station antennas have been developed. Some of them are either sector-beam array or multi-beam array type. In general, each base station should be able to provide omnidirectional coverage, 360° around the base station and having a narrower beam in the elevation. Some base station antennas have been discussed in the next sections.

In this thesis, development of one such antenna has been presented. The work is entirely experimental, starting from the development of individual slot radiator and culminating in a linear array giving a sector-beam of $\sim 120^{\circ}$ coverage. The final antenna is envisaged as a combination of three such arrays arranged around a circle to provide omnidirectional coverage.

1.2 Survey of literature on omni/sector-beam antennas

Microstrip patch Array [1] :

This antenna consists a 2x4 microstrip patch elements sub-array with two or four sub-arrays as shown in Fig. 1.1. The patch element is a broad band microstrip antenna with a parasitic element. This antenna radiates vertical and horizontal polarisation in the 900 MHz band. It has $60-120^\circ$ sector beam patterns in the horizontal plane. A two-element excitation method is used and the elements are excited with different amplitudes and out of phase. The feeder section is composed of two hybrids and a phase shifter. The gain deviation is less than 4 dB within the $60-120^\circ$ beam. The VSWR is less than 1.5 over a frequency bandwidth of 9%.

Printed dipole Array [1] :

This array is composed of 8 or 16 printed dipole elements with a corner reflector as shown in Fig. 1.2. This antenna radiates vertical polarisation in the 900 MHz band. It has 180° sector-beam in the horizontal plane. The corner angle of the reflector is 260° and the reflector size is 0.62 wavelength width. The VSWR is less than 1.2 over a frequency bandwidth of 9%.

Narrow slots of edge of a sectoral cylinder [2] :

A slotted triangular cylinder is used for a base station antenna in mobile communication. The radiating slots cut across three edges of a triangular mast, where the slots in each edge provide one beam of 3 dB beam width of 120° .

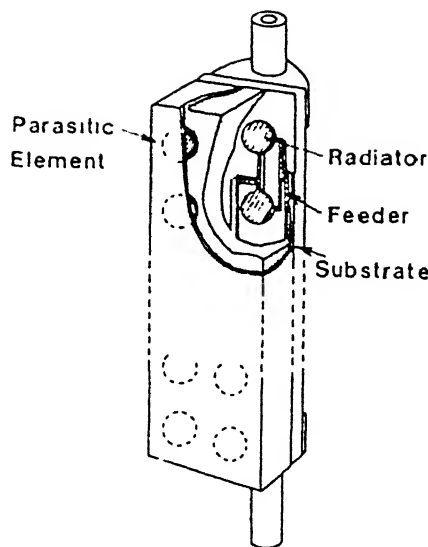


Fig. 1.1 : Configuration of the sector-beam base-station antenna.
(from page 1082, [1])

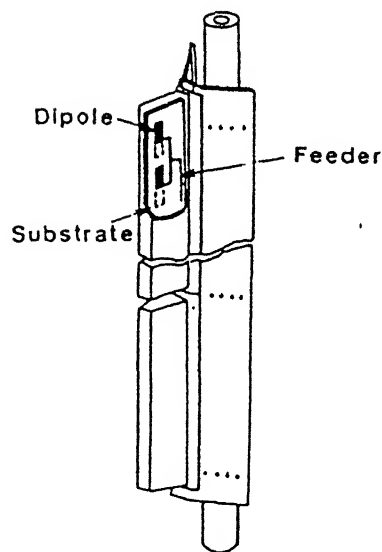


Fig. 1.2 : Configuration of the 180° sector-beam array antenna.
(figure from page 1082, [1])

1.3 MULTI-BEAM ARRAY

The configuration of the multi-beam base-station antenna for land mobile communication is shown in Fig. 1.3. This antenna is composed of 8x8 microstrip patch elements. The patch element is a broad band microstrip antenna with a parasitic element. The antenna operates vertical/horizontal polarisation, and has eight beams within 120° area. The eight beam are switched by a Butler matrix circuit. Microstrip antenna elements and the feed circuits are etched on the same surface. The gain is more than 22 dBi at 900 MHz and the circuit loss is less than 2 dB.

1.4 WAVEGUIDE SLOT ARRAY

A waveguide with an axial sequence of longitudinal slots represents a collinear array, and such arrays are useful as omnidirectional antennas. For this application the waveguide axis will usually be oriented vertically and it is desirable that the maximum radiation occurs in the horizontal plane. This condition can be satisfied by operating the waveguide as a resonant array where all slots are excited in equal phase. The array configuration in a waveguide is not strictly symmetric about the vertical axis and the azimuth pattern shows a certain amount of directivity. The antenna radiates horizontal polarisation.

Fig. 1.4 shows a broad wall, longitudinal shunt-slot array antenna [3] which is operated as a resonant array in the 50 GHz band. In the usual manner, adjacent slots are spaced one-half guide wavelength apart and are offset by equal and opposite

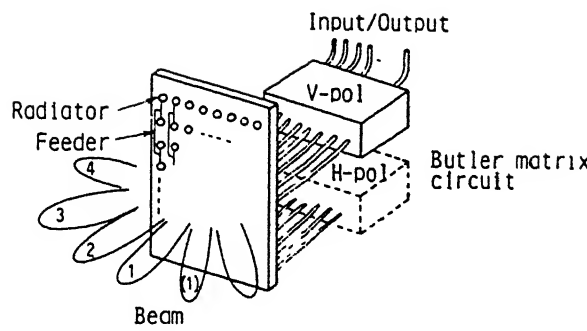


Fig. 1.3 : Configuration of the multi-beam base-station antenna
(from page 1083, [1])

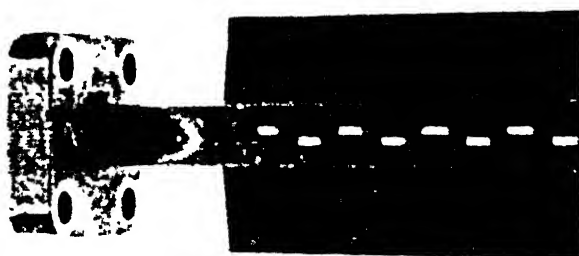


Fig. 1.4 : Slotted-waveguide linear array antenna
for 50 GHz band [3]

amounts from the center line to obtain excitation in equal phase. Eight radiating slots are provided both in the front and rear walls of the waveguide in identical arrangements. The fins attached to the narrow walls assist in achieving the desired omnidirectional pattern in the azimuth plane within a ± 2 dB ripple. The beam width in the elevation plane is approximately 10° , corresponding to a gain of 8 dB.

1.5 CONFIGURATION OF SLOT ARRAY CHOSEN

In recent years microstrip technology has become increasingly important in the design of radiating systems. The low cost, light weight, the simplicity of fabrication and the ability of integration with other printed circuit elements has been strong impetus to this end.

In the present work, a linear array of microstrip line-fed slots are chosen as a sector beam array antenna of 3.2 GHz. The array is fabricated by simple and conventional photo etching technique on a double sided copper-clad glass epoxy substrate. The microstrip-fed slot radiator is chosen as an element of array. The eight longitudinal offset-fed type of slots with uniform spacings of 0.7 times of free space wavelength ($0.7 \lambda_0$) are cut in the ground plane of a microstrip line. The linear array is a broad side with Taylor distribution. A microstrip slot antenna radiates bidirectional, so in order to obtain a unidirectional radiation, a plane reflector sheet is placed below the ground plane and parallel to the slots. The sides of the reflector is made at an angle of 120° as shown in Fig. 1.5, so that three such type of

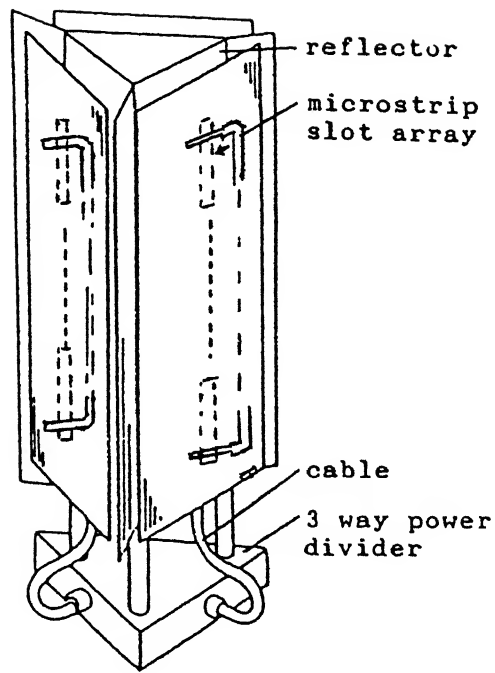


Fig. 1.5 : Three faced array configuration

adjacent linear arrays will give an omnidirectional radiation pattern.

1.6 CONTENTS OF THE THESIS

Chapter 2 contains the design and characterization of microstrip-fed slot antenna, as an element for array fabrication. Chapter 3 consists the mutual coupling measurements among the slots, as required for active impedance calculation in the design of array. In chapter 4 the active impedance computation, matching/feed network design, array fabrication and testing are given. Chapter 5 consists of summary, conclusions and scope for further work.

CHAPTER 2

EXPERIMENTAL STUDY OF MICROSTRIP-FED SLOT

2.1 INTRODUCTION

A rectangular slot in a large ground plane is complimentary to a strip dipole in free-space. The slot impedance (Z_s) is related to the complimentary dipole impedance (Z_d) by a relation known as Booker's relation (Page 369, [4])

$$Z_s \cdot Z_d = \eta^2 / 4 \quad (2.1)$$

Here η is the intrinsic impedance of the free space.

Practical slot radiator can be made on a copper clad dielectric sheet by etching process. A slot in a ground plane with a dielectric support acts slot transmission line. A slot radiator can be treated as a $\lambda/2$ long resonant slot line. The characteristic impedance, Z_0 of a slot transmission line and guide wavelength λ' in the slot line can be obtained by empirical formulae. The following formulae [5] are valid within $0.006 \leq h/\lambda_0 \leq 0.060$, $2.22 \leq \epsilon_r \leq 3.8$ and $0.0015 \leq W/\lambda_0 \leq 0.075$, where h is the dielectric thickness, ϵ_r is the relative dielectric constant and W is the width of the slot.

$$\lambda'/\lambda_o = 1.045 - 0.365 \ln \epsilon_r + \frac{6.3 (W/h) \epsilon_r^{0.945}}{(238.64 + 100 W/h)} - \left[0.148 - \frac{8.81 (\epsilon_r + 0.95)}{100 \epsilon_r} \right] \ln (h/\lambda_o) \quad (2.2)$$

$$Z_o = 60 + 3.69 \sin \left[\frac{(\epsilon_r - 2.22)\pi}{2.36} \right] + 133.5 \ln(10\epsilon_r) \sqrt{\frac{W}{\lambda_o}} + 2.81 \left[1 - 0.011\epsilon_r (4.48 + \ln \epsilon_r) \right] (W/h) \ln(100h/\lambda_o) + 131.1 (1.028 - \ln \epsilon_r) \sqrt{h/\lambda_o} + 12.48 (1 + 0.18 \ln \epsilon_r) \frac{W/h}{\sqrt{\epsilon_r - 2.06 + 0.85 (W/h)^2}} \quad (2.3)$$

Since the resonant slot radiator is approximately $\lambda'/2$ long, we can use these formulae to arrive at initial values of the slot radiator, given the dielectric constant of the substrate and thickness. Actual dimensions will be around these values hence can be experimentally determined. Because of radiation loss in a resonant structure and the fringing current effects at the sharped ends of the slot, the actual resonant length is somewhat smaller than $\lambda'/2$. This is experimentally determined by making measurements on an initial slot radiator made using the approximate formulae and then subsequently calculating the correctness required for the dimension based on the measured results.

2.2 SLOT GEOMETRY

A microstrip-fed slot antenna, shown in Fig.2.1 is fabricated by simple photo etching techniques on copper clad glass epoxy substrate. The slot is etched in the ground plane and is excited by a microstrip line. The feed point is offset from the center of the slot with an open circuit tuning stub. The width of the feeding microstrip line and tuning stub is so determined that the characteristic impedance of the line is 100Ω . The microstrip line is transformed to a 50Ω line with the help of a quarter wave microstrip line transformer. To achieve unidirectional radiation, a plane reflector sheet of the size of ground plane is placed below the slot at an appropriate distance.

2.3 SLOT CHARACTERISTICS

A radiating slot in the ground plane of a microstrip line appears as a discontinuity impedance Z in series with the microstrip line, as shown in Fig. 2.2. The series impedance Z [6] can be calculated from the reflection coefficient on the microstrip line using the formulae

$$Z = Z_c \cdot \frac{2R}{1-R} \quad (2.4)$$

For available substrate materials and thickness, center-fed transverse slots exhibit high values of normalized (to 50Ω) radiation impedance [6,7,8]. This was considered a very serious obstacle for practical applications of microstrip slot radiators. Typical normalized values of impedance at resonance for the center-fed transverse slot backed by PTFE substrate of relative

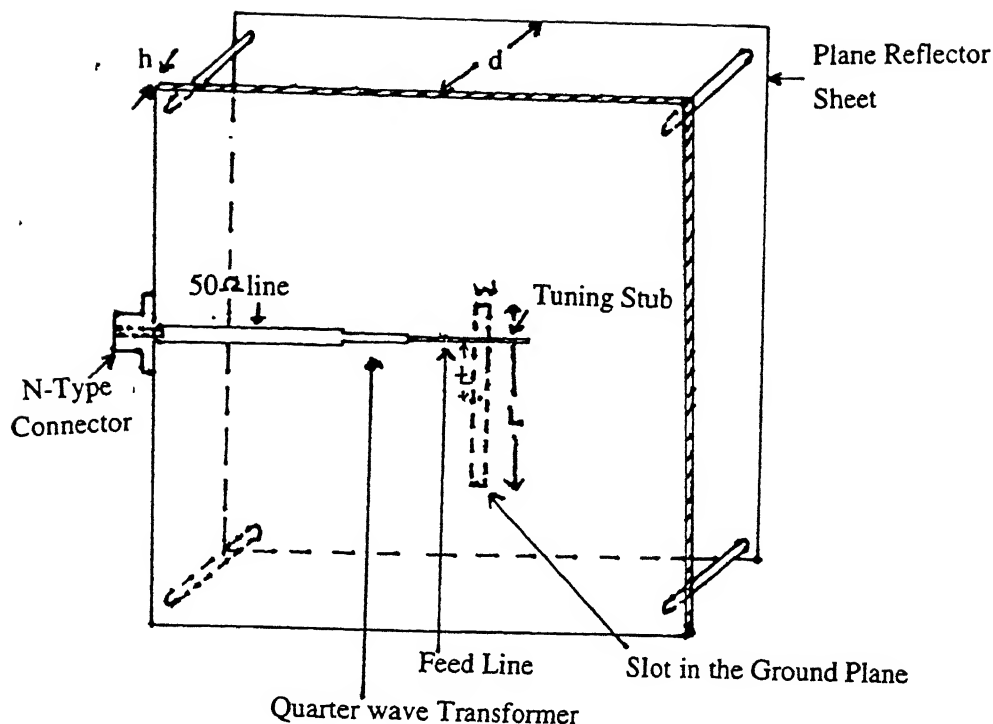


Fig. 2.1 : Configuration of microstrip-fed slot antenna

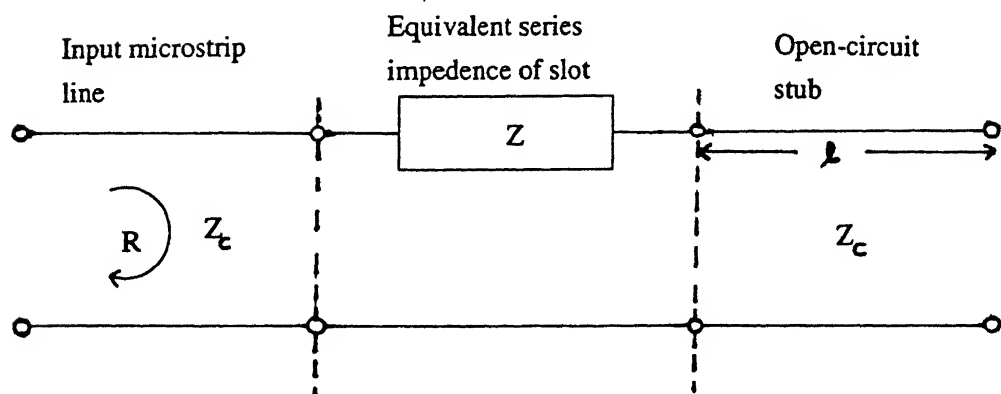


Fig. 2.2 : The equivalent circuit of a slot in the ground plane of a microstrip line [6]

dielectric constant, $\epsilon_r = 2.2$ are around 12 [6,9,10]. In order to overcome this difficulty Yoshimura [11] shifted the feed point from the center of the slot (offset-fed) and short circuited the microstrip feed through the dielectric substrate with the slot side, which is located farther from the feed input. A similar technique of offset feed to the slot was used by Pozar [6], the only difference being that the microstrip line was terminated by an open-circuited tuning stub. In both the cases the offset of the feed point leads to a perfect impedance matching in a narrow frequency band. The input impedance of center-fed slots and offset-fed slots as a function of length and feed point is reported by Yoshimura [11]. Rigorous analysis of the microstrip slot by the method of moments was performed by Pozar [6].

A typical resonant Z_{in} characteristics of a microstrip-fed cavity backed slot as a function of offset is given in Fig. 2.3, which is taken from [9]. Similarly the variation of normalized Resistance (R to 50Ω) at resonance for various offset values (t) are calculated, from the curve of slot impedance variation versus frequency (of various offset values) [10], and shown in Fig. 2.4. The curve shows that the Z_{in} roughly follows a $\cos^2\theta$ shape, except at the ends. The variation of normalized resistance with respect to offset values can be expressed by the following empirical relation.

$$R = A \cos^2 \left[\left(\frac{t}{l} \right) \cdot \frac{\pi}{2} \right] \quad 2.5$$

Here $A = 12.5$ and $l = L/2$.

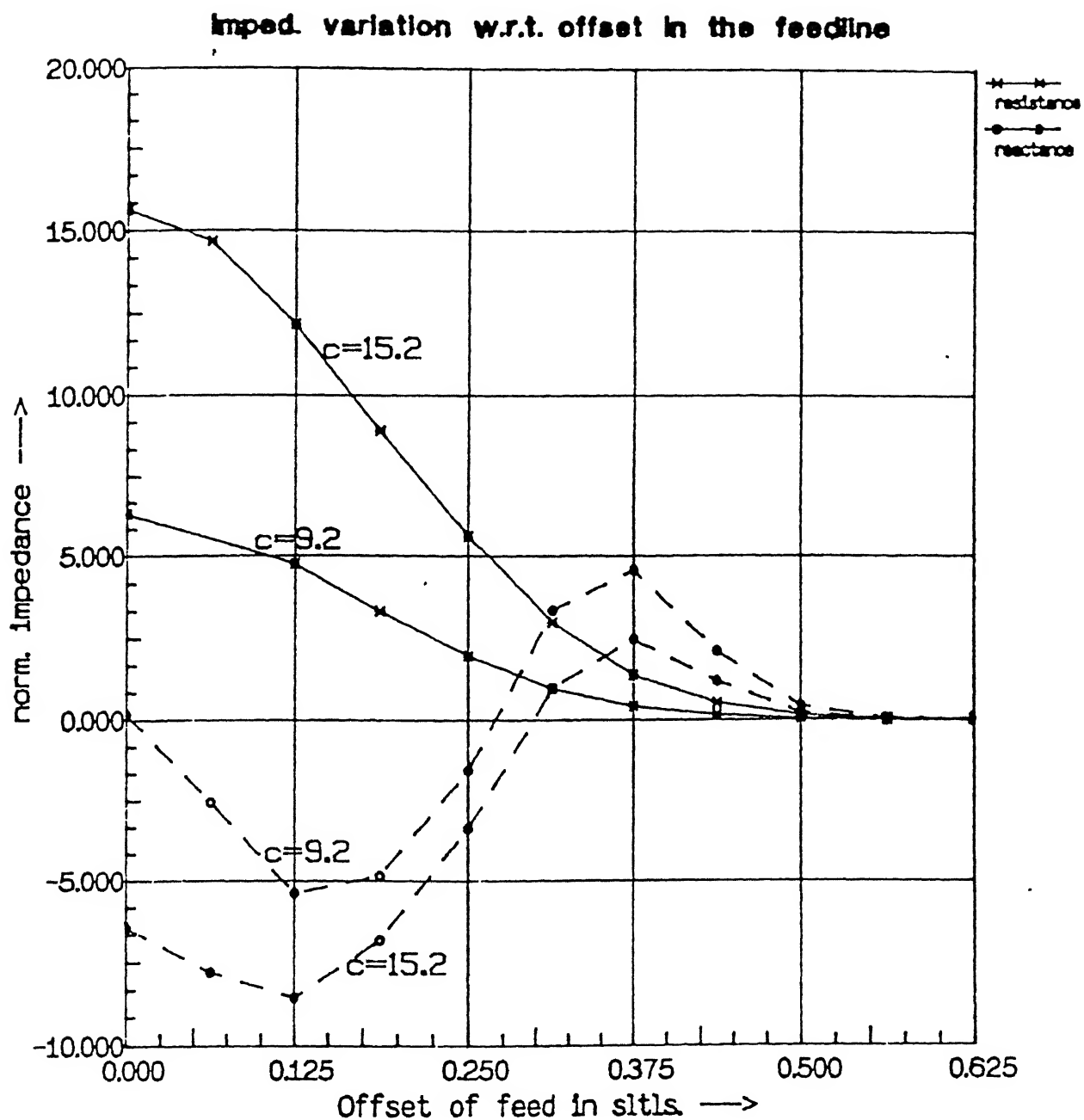


Fig. 2.3 : Normalized equivalent impedance of the cavity backed slot versus offset of the feedline (C = cavity depth in mm)[9]

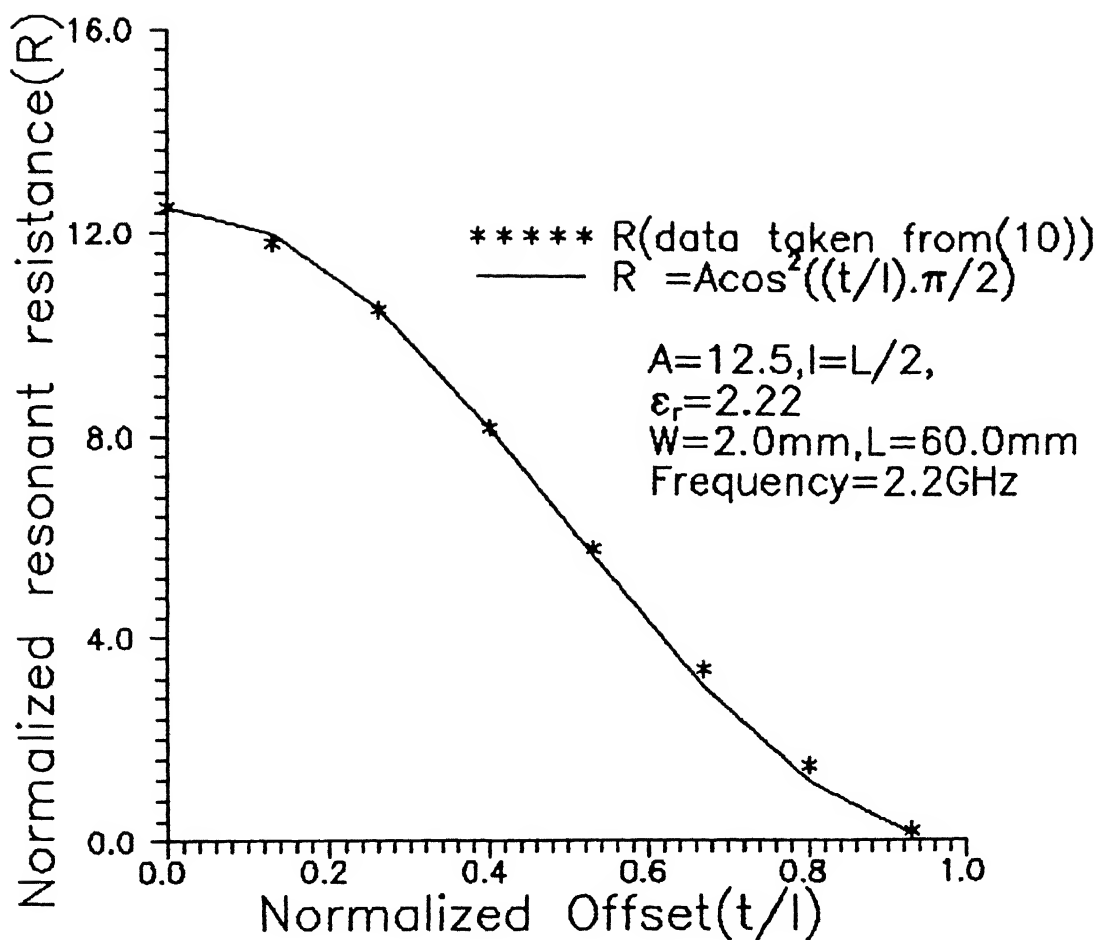


Fig. 2.4 : The normalized resonant resistance versus normalized offset of a micro-strip-fed slot antenna

A microstrip-fed slot radiates bidirectionally which is not desirable in many cases. In order to obtain the unidirectional radiation, various techniques have been reported. The cavity backed slot antenna, to achieve unidirectional radiation, has been analysed by Sridhar [9]. It is reported that as the cavity depth increases the resonant frequency of the slot shifts towards the lower frequencies, which is equivalent to the increasing the capacitive loading to the antenna. Below certain cavity depth \approx 12.2 mm (to 11 GHz) the antenna resonant frequency is shifted to higher frequency side. Normalized equivalent impedance of the cavity backed slot with respect to the variation in the offset of feed line is also reported.

In order to obtain unidirectional radiation, Yoshimura [11] placed a plane reflector sheet of the size of ground plane on the side of the dielectric substrate parallel to the slot surface. He observed that the slot with the reflector is almost short-circuited, when the slot-to-reflector spacing is near even multiples of $1/4$ free-space wavelength (i.e. $n \cdot \frac{\lambda}{4}$, n-even), but it is close to resonance when it is near odd multiples of $1/4$ free-space wavelength. It is also reported that the optimum spacing between the slot and the reflector is nearly one-quarter-space wavelength. The beam width, maximum side lobe level and the front-to-back ratio of the matched slots are similar to a complimentary dipole antenna.

Thus, it can be concluded that the slots can be matched with a microstrip line, depending upon appropriate length, width and

feed point. Similarly unidirectional, radiation can be achieved either by metallic cavity backing or using a plane reflector by placing at appropriate depth. However, the plane reflector spacing of $\lambda/4$ works well for broadside arrays, but may lead to the excitation of parallel plate waveguide modes in a scanning array. The effect of radiations from the sides have not been analysed so far. At present no rigorous analysis of reflector backed slot is available in the literature.

2.4 APPROXIMATE DESIGN

As, a radiating slot is complementary to a dipole antenna, the bandwidth or selectivity characteristics of a slot antenna are the same as for complementary dipole. Thus widening a slot increases the bandwidth of the slot antenna, the same way as increasing the thickness of a dipole antenna (Page 370, [4]). Therefore, to design a radiating slot, at 3.2 GHz ($\lambda_0 = 93.75$ mm), fed by microstrip line on a glass epoxy substrate ($\epsilon_r = 3.8$, $h = 1.6$ mm), the width of the slot is selected as 3.0 mm, using equation (2.2), (2.3) the Z_0 of the slot is 160.27 ohms and the guide wavelength, λ' , in the slot is 75.92 mm. As the reactance of a dipole is seen sensitive of a/λ_0 , a is the radius of the dipole. As a/λ_0 increases, the resonance occurs at shorter lengths (Page 302, [12]). Therefore, for a slot of width (W) 3.0 mm, the slot length (L) 34.5 mm ($0.454\lambda'$) is chosen.

The offset (t) 14.45 mm is evaluated by equation (2.5), taking the normalized resistance (to 50 Ω) value of a center-fed slot as 16 [7]. Hence a slot of $W=3.0$ mm, $L=34.5$ mm and $t=14.45$ mm

is etched in the ground plane of a microstrip line of characteristic impedance 50Ω on a copper clad glass epoxy substrate ($\epsilon_r = 3.8$, $h = 1.6$ mm) using a photo etching technique. The feed is short circuited through the dielectric substrate with the slot longer side, which is located farther from the feed input. No matching element is used. The size of the ground plane is 150 mm x 150 mm.

The S_{11} measurements, magnitude and phase, of slot are carried out on a HP-8410 Network Analyzer in the frequency range 2.0 - 4.0 GHz. The impedance variation of the slot with respect to frequency is shown in Fig. 2.5. In order to obtain the unidirectional radiation, a plane reflector sheet is placed below the ground plane and parallel to the slot. The size of the reflector is same as of the the ground plane. Fig. 2.5 to 2.11 shows the variation of input impedance as a function of frequency and slot-to- reflector spacings. The impedance variation of slot with respect to, slot-to-reflector spacing at 3.2 GHz is shown in Fig. 2.12. It is observed that the reactive part of input impedance remains inductive (Fig. 2.5 to 2.11) and at 3.2 GHz the maximum resistance is observed when slot-to-reflector spacing is 19.2 mm (Fig. 2.12). Therefore it is decided that for further study of slot, instead of shorting the strip, an open circuited tuning stub is to be used and the slot-to-reflector spacing is to be 20.0 mm.

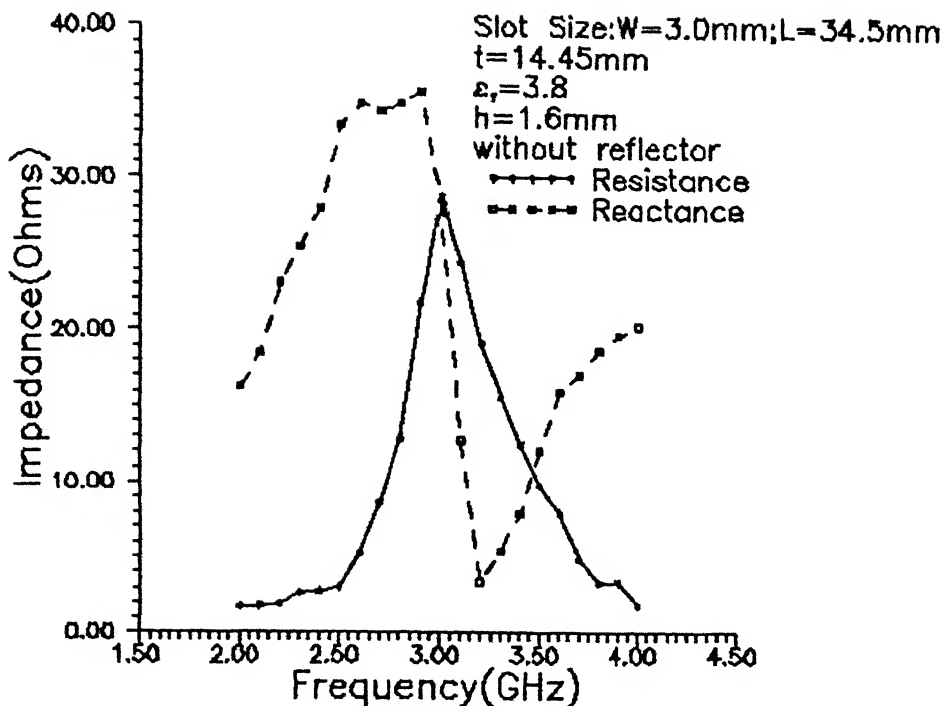


Fig. 2.5 : Input impedance versus frequency of microstrip-fed slot antenna

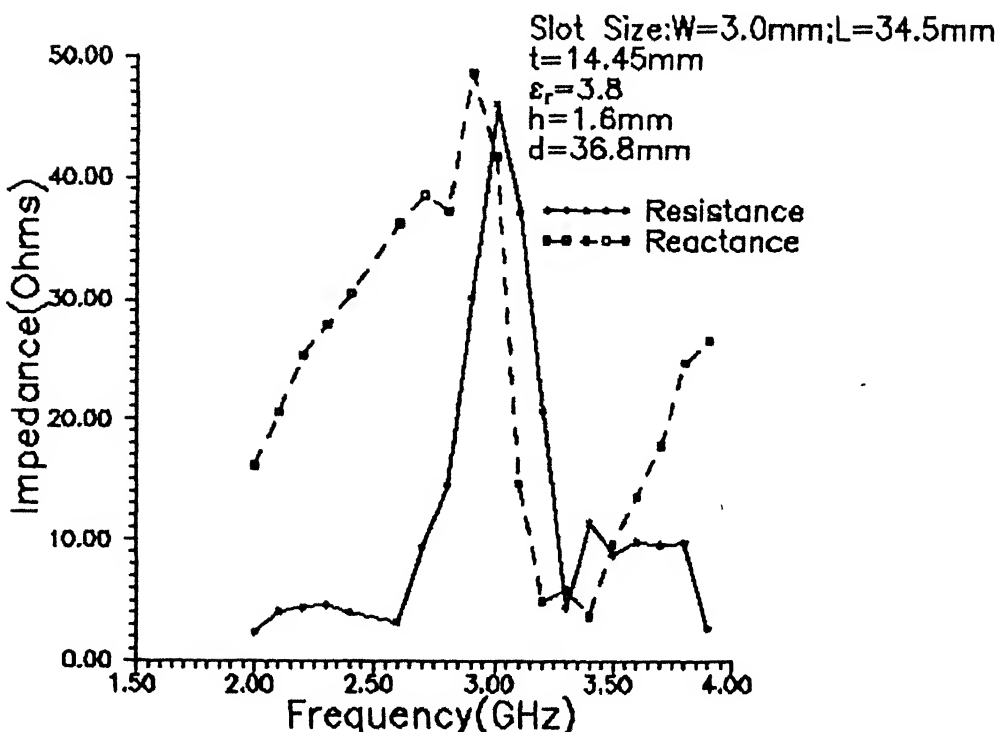


Fig. 2.6 : Input impedance versus frequency of microstrip-fed slot antenna

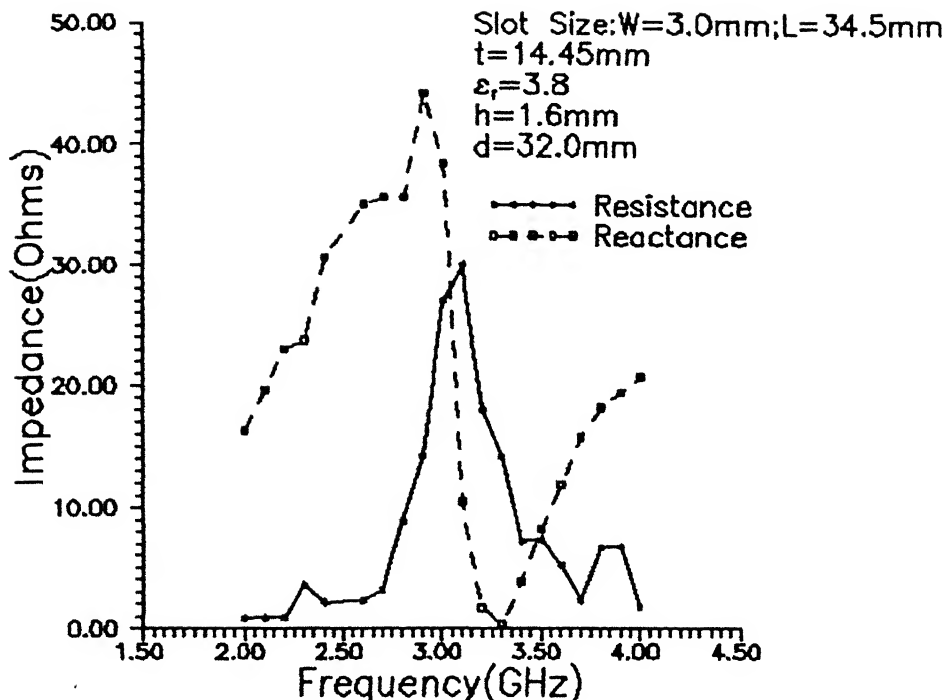


Fig. 2.7 : Input impedance versus frequency of microstrip-fed slot antenna

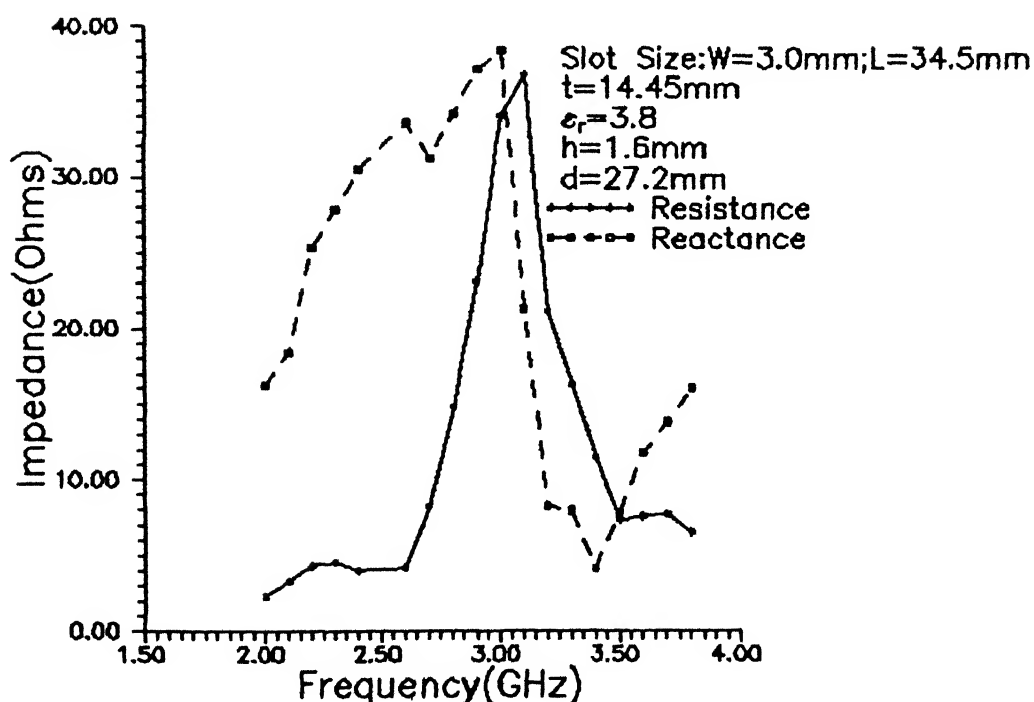


Fig. 2.8 : Input impedance versus frequency of microstrip-fed slot antenna

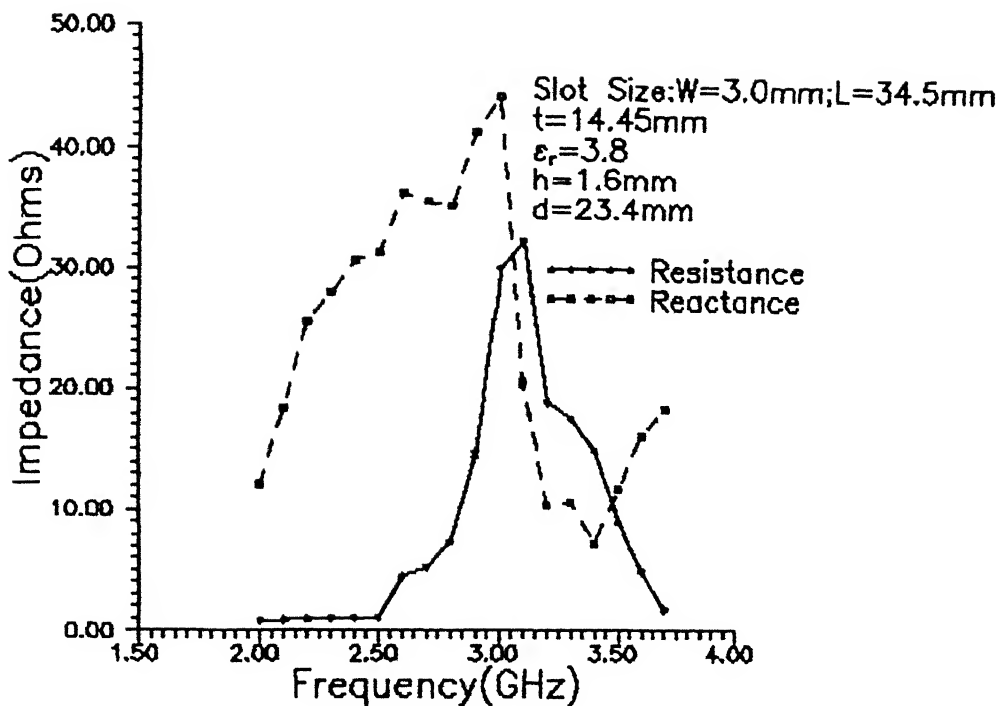


Fig. 2.9 : Input impedance versus frequency of microstrip-fed slot antenna

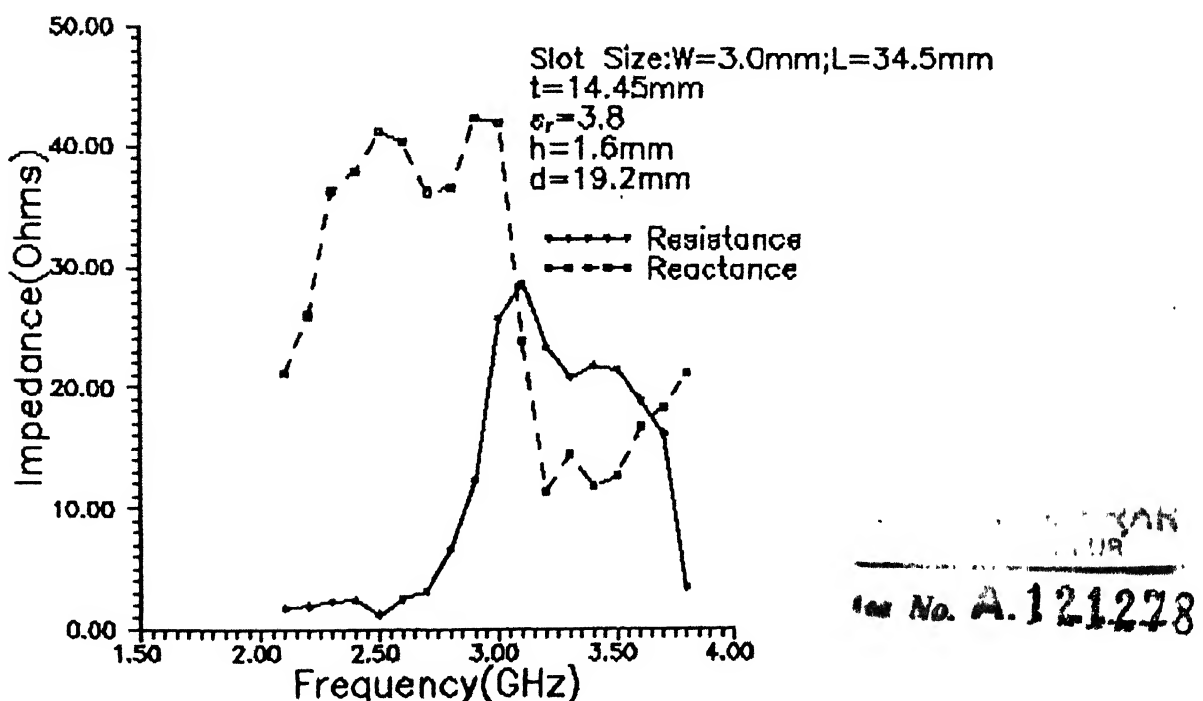
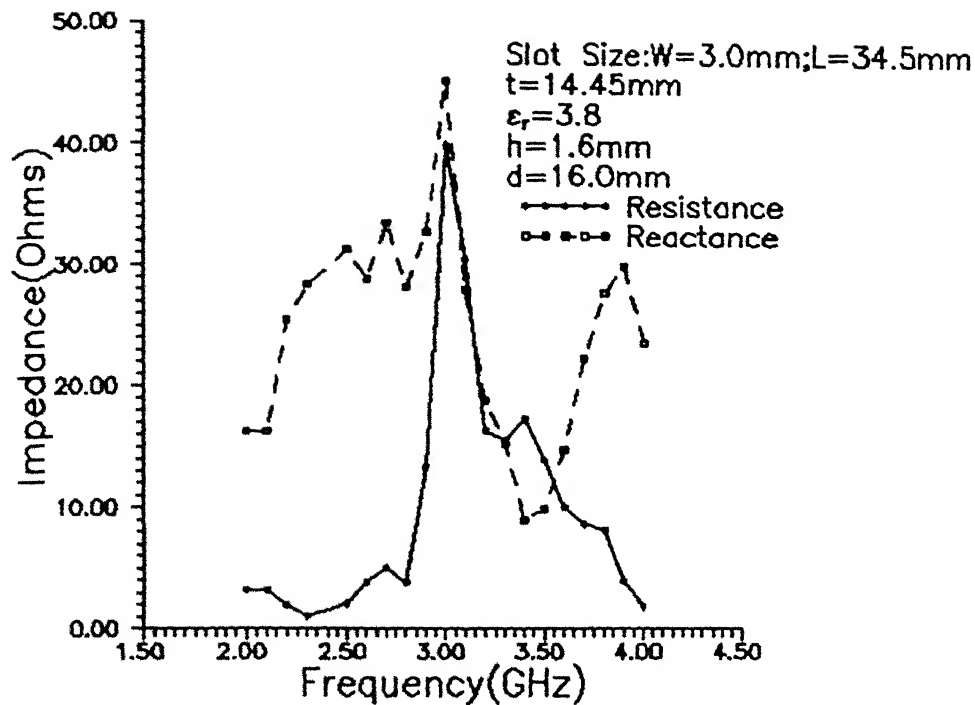
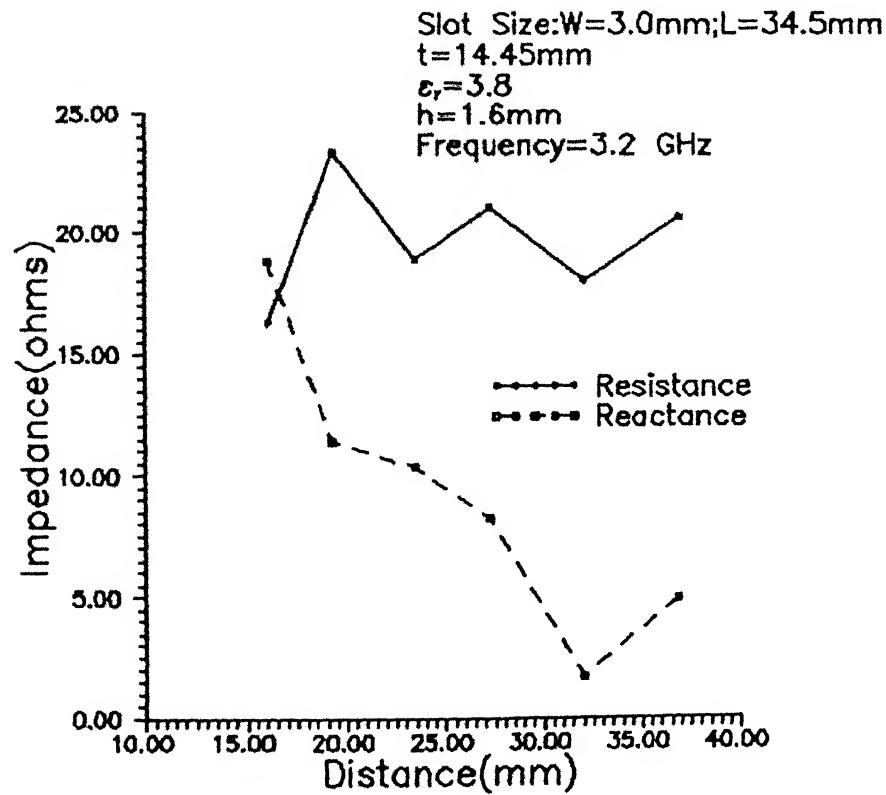


Fig.2.10 : Input impedance versus frequency of microstrip-fed slot antenna



2.11 : Input impedance versus frequency of microstrip-fed slot antenna

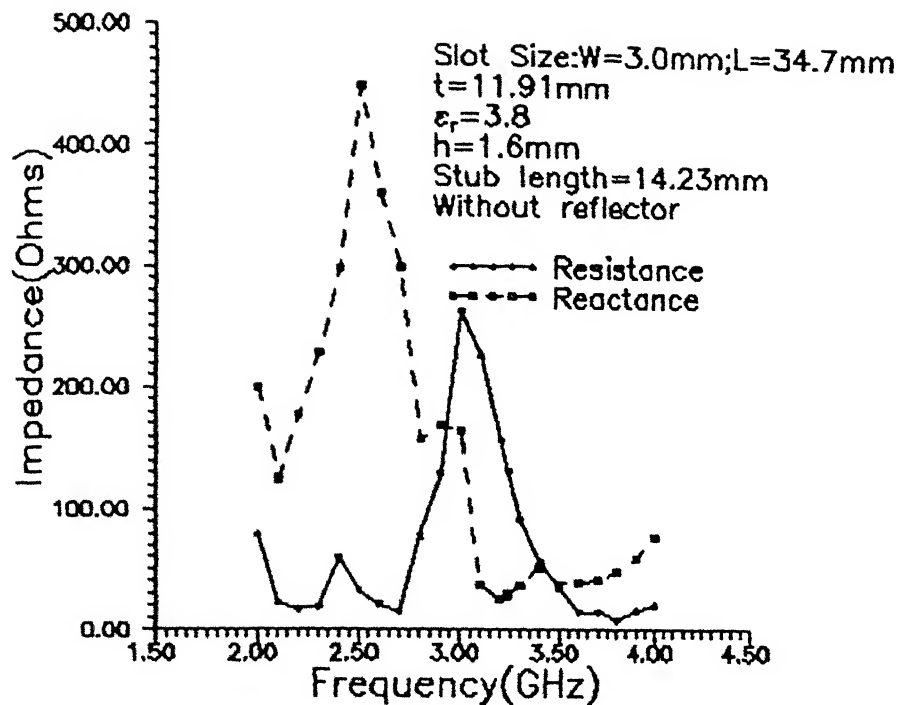


2.12 : Input impedance versus slot-to-reflector spacing at 3.2 GHz

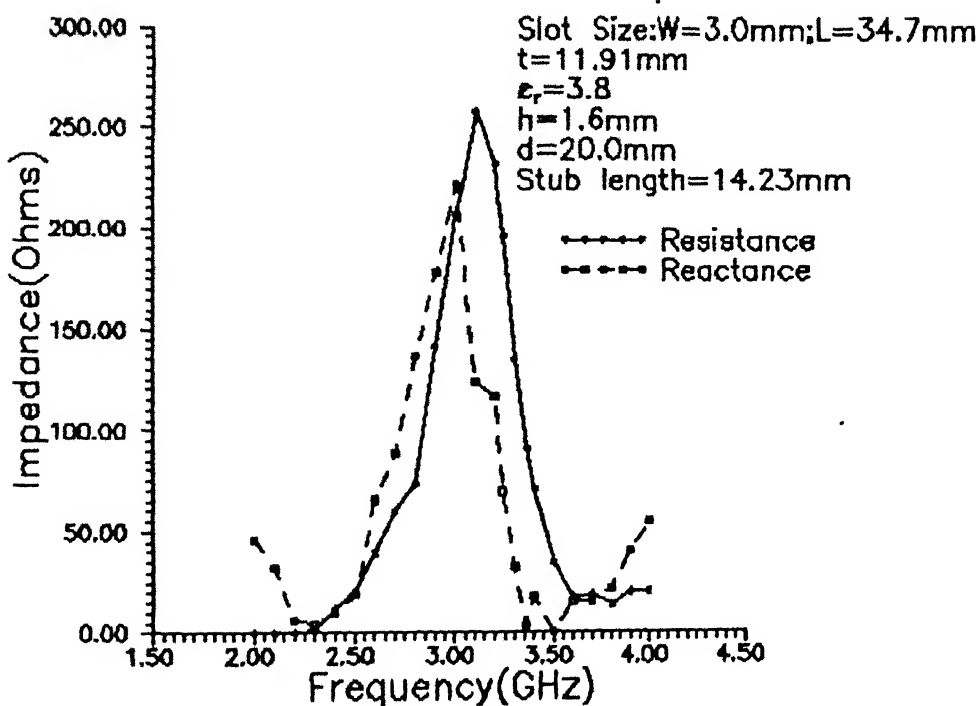
MODIFICATION

The Fig. 2.12 shows that the input impedance of the slot at GHz is $23.38 + j11.40$ ohms. Since the offset for 50Ω line is the edge of the curve (Fig. 2.4), hence the chances of error more. Therefore, for further study, to make the offset more towards the center, the characteristic impedance of feed line is taken as 100Ω . The offset for this line is calculated, wrongly, 1.91 mm. Hence a slot is fabricated on a glass epoxy substrate with the dimension $W = 3.0$ mm, $L = 34.7$ mm and $t = 11.91$ mm. This is fed by a microstrip line of characteristic impedance Ω , width (w_f) 0.84 mm with an open circuited microstrip line of length 14.23 mm, width (w_s) 0.84 mm. The 100Ω line is transformed to a 50Ω coax transition using a quarter wave microstrip line transformer. The length of the transformer is 18 mm of width (w_t) 1.85 mm.

The S_{11} measurements are carried out with the help of HP-8410 Network Analyzer. The observations are made without reflector and with the reflector at $d = 20.0$ mm. The impedance variation with respect to frequency is shown in Fig. 2.13 and 2.14. It is observed that the input impedance of the modified design is $20.08 + j3.42$ ohms (Fig. 2.14) at 3.36 GHz. The reactive part remains inductive, despite the tuning stub. The reason for this may be that 50Ω connector is straight on the quarter wave transformer, so it may be that proper transformation of 50Ω is not taking place and the connector pin is also producing an additional inductive effect. Hence it is decided that for smooth



g.2.13 : Input impedance versus frequency of microstrip-fed slot antenna



g.2.14 : Input impedance versus frequency of microstrip-fed slot antenna

transition a 50Ω microstrip line is to be made between trans-
former and coax transition.

5 FINAL CONFIGURATION

The input impedance of the modified design is $91.08 + j3.42$ Ω at 3.36 GHz. So to make the slot resonant around 3.2 GHz, the length of the slot is increased and made to 35.0 mm, as lengthening of half-wavelength slot makes it more capacitive (Page 9-[4]). The resistive part of the impedance is approximately equal to the characteristic impedance of the feed line. Hence, offset is taken as 12.0 mm (a round off value of 11.91 mm). The slot is fed by 100Ω line with an open circuited stub as earlier. 50Ω micro-strip line is also made between the quarter wave transformer and 50Ω coax connector. The slot-to-reflector spacing is 20.0 mm.

The S_{11} measurements are taken on a HP-8410 Network Analyzer. The observed S_{11} is -29.0 dB at 3.3 GHz and 10 dB down bandwidth is 3.2 - 3.39 GHz. So to get the bandwidth between 3.0 - 3.3 GHz, the slot length is now increased by trial methods as explained in the following steps.

The slot length is increased by 0.5 mm from the offset side. Subsequently the slot length has become 35.5 mm and $t = 11.75$ mm. The measurement S_{11} is -37.5 dB at 3.30 GHz and 10 dB bandwidth is 3.18 - 3.38 GHz.

Now slot length is increased by 1.0 mm from the other than the offset side ($L = 36.5$ mm, $t = 12.25$ mm) The measured results are $S_{11} = -18.0$ dB at 3.24 GHz and bandwidth is 2.97 - 3.35 GHz.

To get less S_{11} , the offset side is increased further by 0.5 mm ($L = 37.0$ mm, $t = 12.0$ mm) The S_{11} is -30.0 dB at 3.24 GHz and bandwidth is 3.0 to 3.3 GHz.

Now to get the minimum S_{11} at 3.2 GHz, the slot length is further increased by 0.5 mm on the other than offset side of the slot The slot length has become 37.5 mm and $t = 12.25$ mm The measured $S_{11} = -16.5$ dB at 3.21 GHz Bandwidth is 3.03 - 3.3 GHz.

The slot length is further increased by 0.5 mm from the offset side. So $L = 38.0$ mm, $t = 12.0$ mm The S_{11} is -17.5 dB at 3.21 GHz and bandwidth is 3.05 - 3.30 GHz

Now the slot is in the required bandwidth range of 3.0 - 3.3 GHz. However, to obtain S_{11} minimum the slot length is further increased by 0.5 mm at the offset side. The length has become 38.5 mm and $t = 11.75$ mm The S_{11} is -18.5 dB at 3.21 GHz and the bandwidth is 3.04 - 3.30 GHz.

Further the slot length is increased by 0.5 mm from the offset side The slot length is now 39.0 mm, $t = 11.5$ mm and measured S_{11} is -18.5 dB at 3.20 GHz The bandwidth is 3.05 - 3.28 GHz. As the S_{11} is not improving further The final dimensions of the slot is selected as

$W = 3.0$ mm, $L = 39.0$ mm, $t = 11.5$ mm and $d = 20.0$ mm.

The S_{11} measurements are taken on a HP-8410 Network Analyzer. As the reference plane of measurement is at the coax transition. Hence for the impedance evaluation at the slot, the S_{11} is transformed from the reference plane to the slot using the following relation

$$\Gamma_{\text{at slot}} = |\Gamma| \cdot e^{[j\theta + 2(\gamma_1 l_1 + \gamma_2 l_2 + \gamma_3 l_3)]} \quad (2.6)$$

Hence, $|\Gamma|e^{j\theta}$ is the reflection coefficient at the reference plane. γ_1 , γ_2 and γ_3 are the propagation constant for 50Ω , 70.7Ω and 100Ω microstrip lines. The $l_1 = 41.7 \text{ mm}$, $l_2 = 13.88 \text{ mm}$ and $l_3 = 14.23 \text{ mm}$ are their lengths respectively. In general $\gamma = \alpha + j\beta$, here α is the attenuation constant.

$$\alpha = \frac{\pi\sqrt{\epsilon_r} \tan\delta}{\lambda_0} \quad (2.7)$$

as the substrate is lossy and the loss tangent, $\tan\delta = 1/60$.

And $\beta = 2\pi/\lambda_g$ (2.8)

Here $\lambda_g = \lambda_0/\sqrt{\epsilon_{\text{eff}}}$.

During impedance evaluation at the slot, the impedance offered by the open-circuited stub of length 14.0 mm is subtracted.

The Fig. 2.15 shows the $|S_{11}|$ variation of slot versus frequency. The impedance variation of the slot with respect to frequency is shown in Fig. 2.16. It is observed that the slot is resonant at frequency 3.23 GHz and the V.S.W.R. is less than 1.31 in the frequency range of $3.0 - 3.3 \text{ GHz}$.

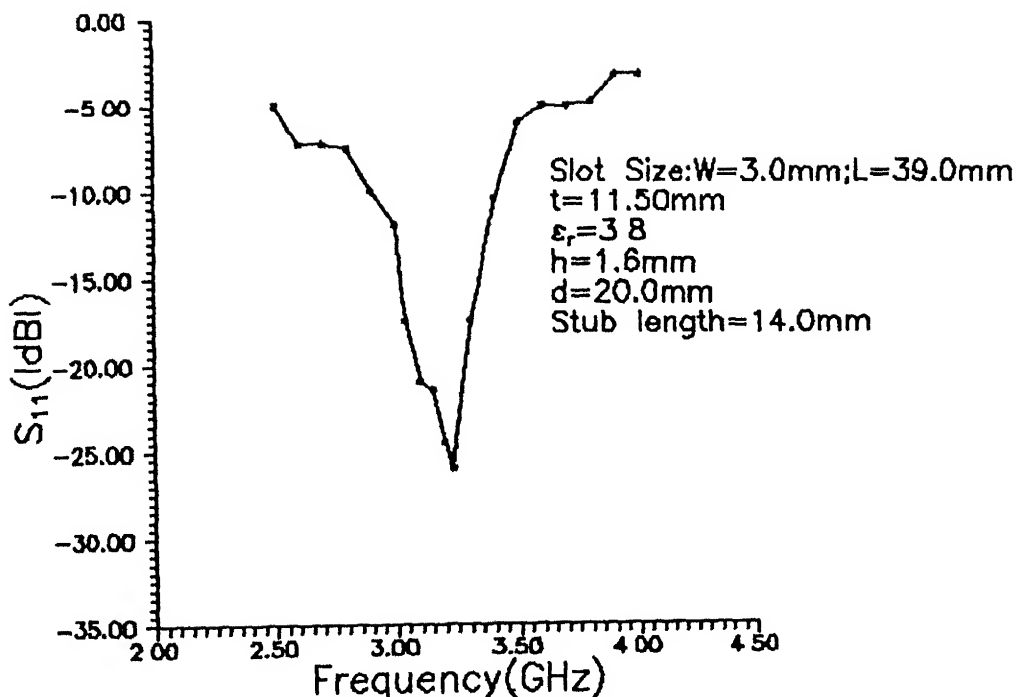


Fig 2.15 · The magnitude of S_{11} of microstrip-fed slot antenna

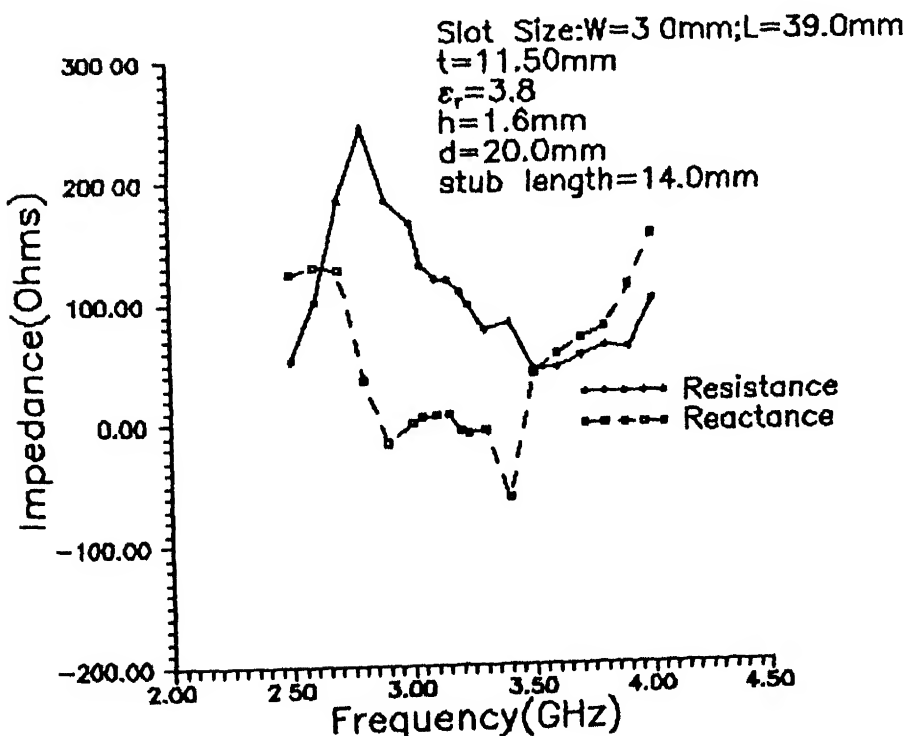


Fig.2.16 : Input impedance vs frequency of microstrip-fed slot antenna

The radiation pattern of the slot is measured at frequency 3.2 GHz Fig 2.17, 2.18 shows the E-plane and H-plane radiation patterns of the slot respectively, when the reflector is placed at $d = 20.0$ mm on strip side. Similarly Fig 2.19, 2.20 shows the E-plane and H-plane radiation pattern of the slot respectively, when reflector is placed at $d = 20.0$ mm on the slot side. In both the cases it is observed that besides the main beam, significant side lobes are present. The reason for this interference may be that as the radiations are measured in the laboratory, where the radiations are scattered back by the surrounding equipments as well as the radiations from the sides of the reflector.

2.7 CONCLUSION

It is concluded that a microstrip-fed slot (offset-fed) on a glass epoxy substrate with a reflector ($d = 20.0$ mm) is resonant at 3.23 GHz, if the slot length is $0.513\lambda'$. As the measured VSWR is less than 1.31 in the frequency range 3.0-3.3 GHz, the antenna can be utilized as an element for the development of an array in this frequency range. However, the radiation pattern of antenna is having interferences, the directivity of the element cannot be evaluated correctly. Therefore, after studying the mutual coupling between the elements and depending upon the desired directivity, the array can be fabricated using the final configuration of the antenna.

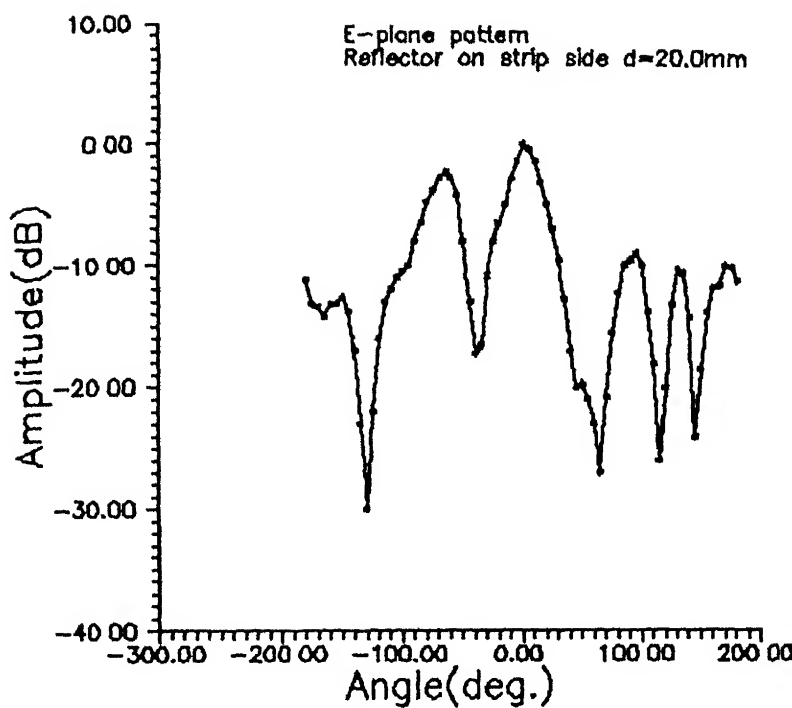


Fig 2.17 · E-plane radiation pattern of final element

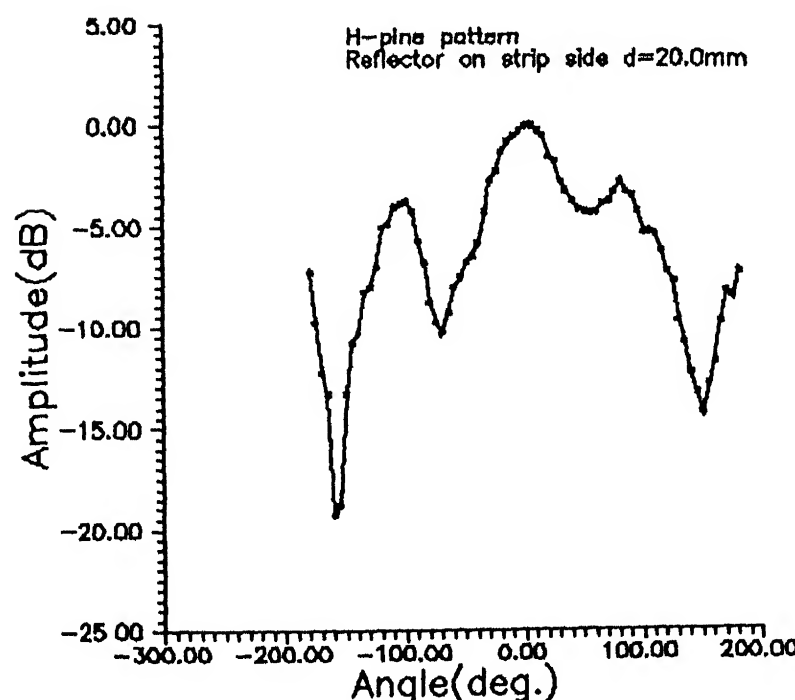


Fig 2.18 H-plane radiation pattern of final element

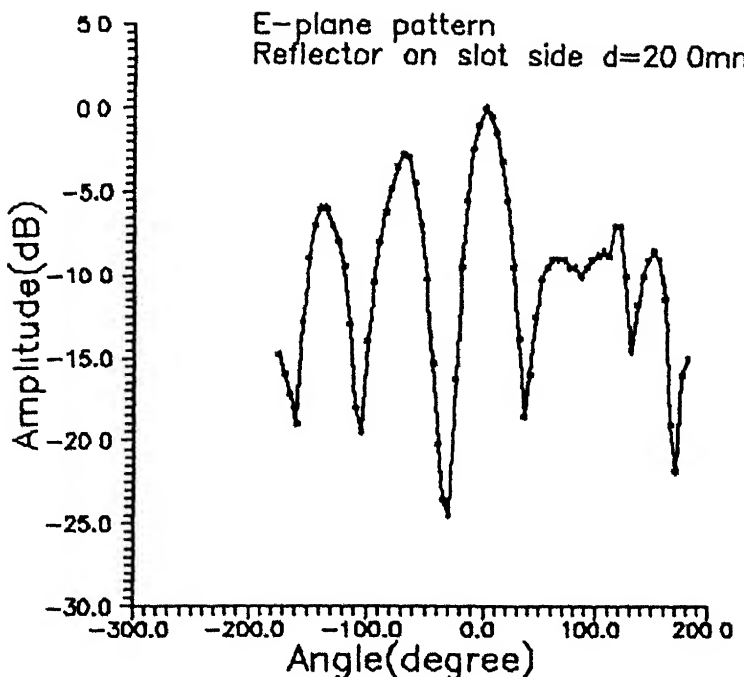


Fig 2.19 E-plane radiation pattern of final element

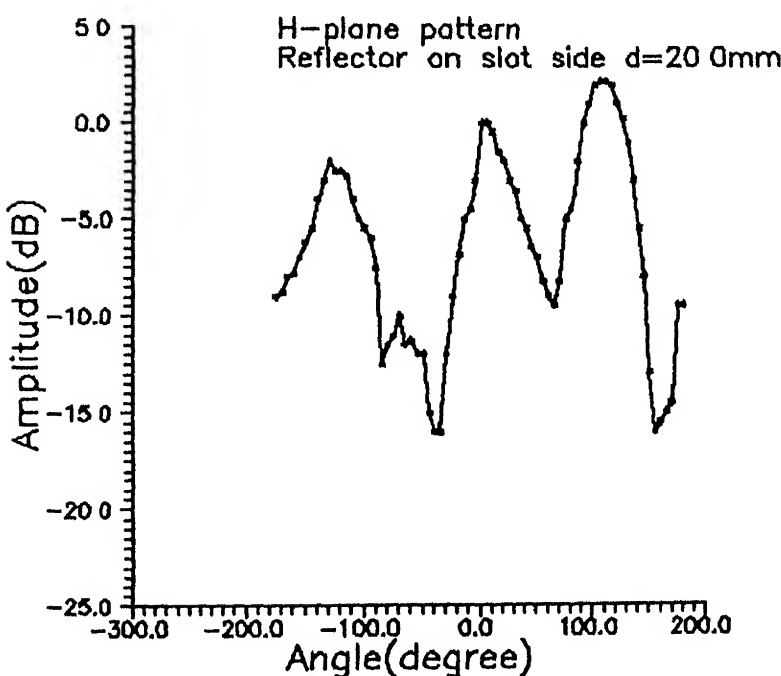


Fig 2.20 : H-plane radiation pattern of final element

CHAPTER 3

MUTUAL COUPLING EVALUATION

3.1 INTRODUCTION

In an array application the mutual coupling between neighbouring elements becomes important since it degrades the pattern required. The active impedance of an element is different from its self impedance due to mutual coupling. The mutual coupling of microstrip-fed slot elements can be caused mainly due to interaction through free space radiation and interaction by surface waves which propagate along the dielectric substrate. In the present case a metallic sheet reflector at a distance below the ground plane is also used so the interaction of these waves and the waves reflected by the sheet or due to the images of slots formed on the sheet, becomes more complicated. The coupling effects of such type of elements is not available in the literature, so it became necessary to investigate experimentally the mutual coupling effects between elements. The self and mutual admittances are measured experimentally and used for the design of the array configuration, in order to achieve the following two objectives :

Attain the radiating current distribution needed to produce a desired pattern, and

Achieve an input match at the design frequency.

3.2 MUTUAL COUPLING MEASUREMENT SET-UP

To study the mutual coupling between elements, the three microstrip-fed slots of dimensions, $W = 3.0$ mm, $L = 39.0$ mm, $t = 1.5$ mm, offset-fed by a 100Ω microstrip line with open-circuited stubs of length 14.0 mm are etched, at a distance(s) of $0.7\lambda_0$ between each elements (the elements spacing is same as required for array design), on a copper clad glass epoxy substrate ($\epsilon_r = 3.8$, $h = 1.6$ mm) Each 100Ω microstrip line is transformed to a 50Ω microstrip line via a quarter wave microstrip line transformer and then to a 50Ω coax transition. The reflector is placed at a distance $d = 20.0$ mm below the ground plane, as shown in Fig. 3.1.

The S-parameter measurements between the slots are carried out on a HP-8410 Network Analyzer As the coupling effects are due to space and surface waves, as well as the interaction of these waves with the reflected waves (due to reflector) so the S-parameter measurements are carried out in two ways :

- . S-parameters are measured without reflector (free space measurement) and
- . S-parameters are measured with the reflector kept at a distance $d = 20.0$ mm.

3.2.1 Measured Results

The S_{11} is measured at 3.1-3.3 GHz, as the reflection coefficient is seen at port 1, with two other slots are shorted with the ground plane. The magnitude and phase of S_{11} with respect to frequency is shown in Fig. 3.2 and 3.3, respectively. It is

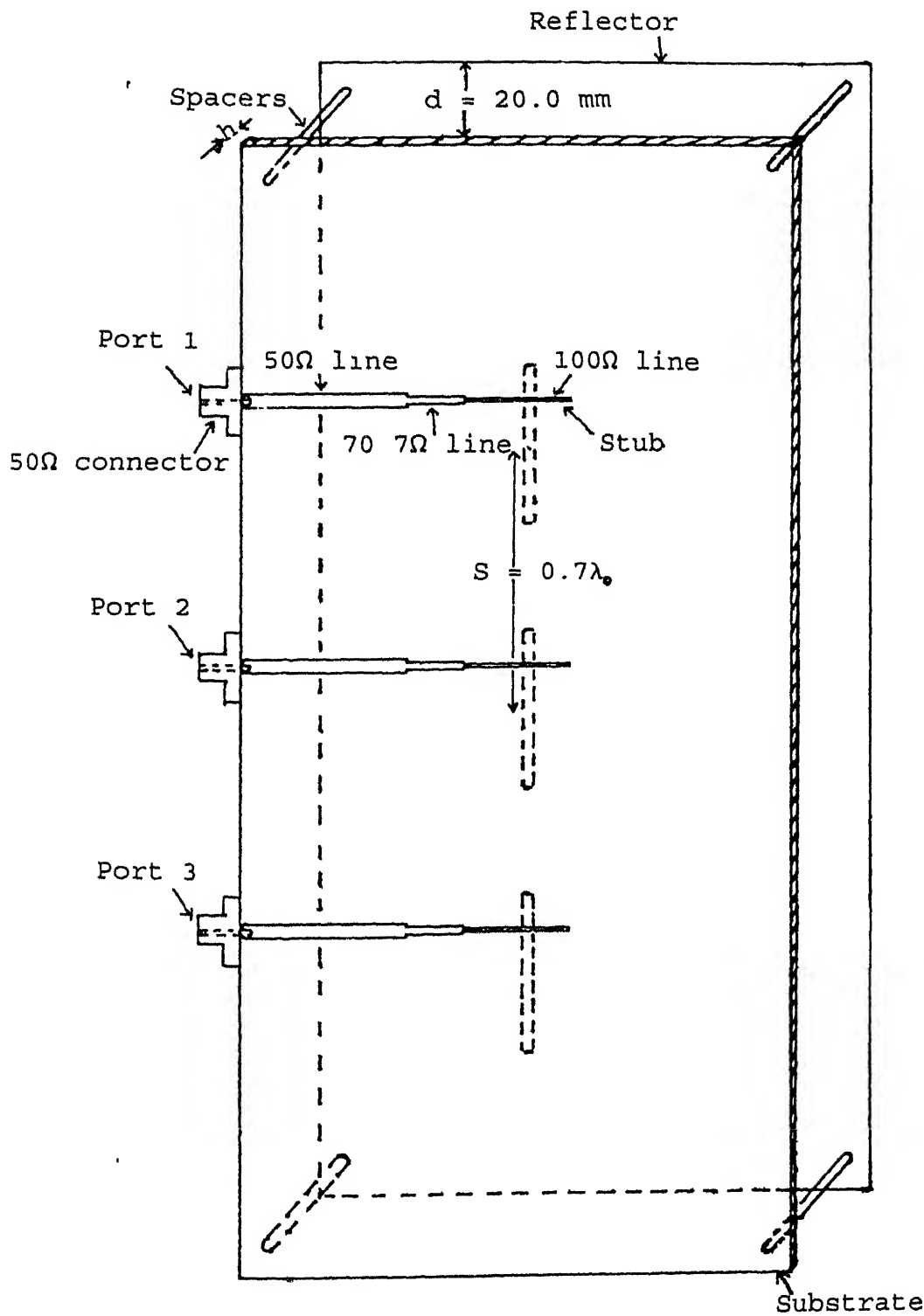


Fig. 3.1 : Configuration of three microstrip-fed slots

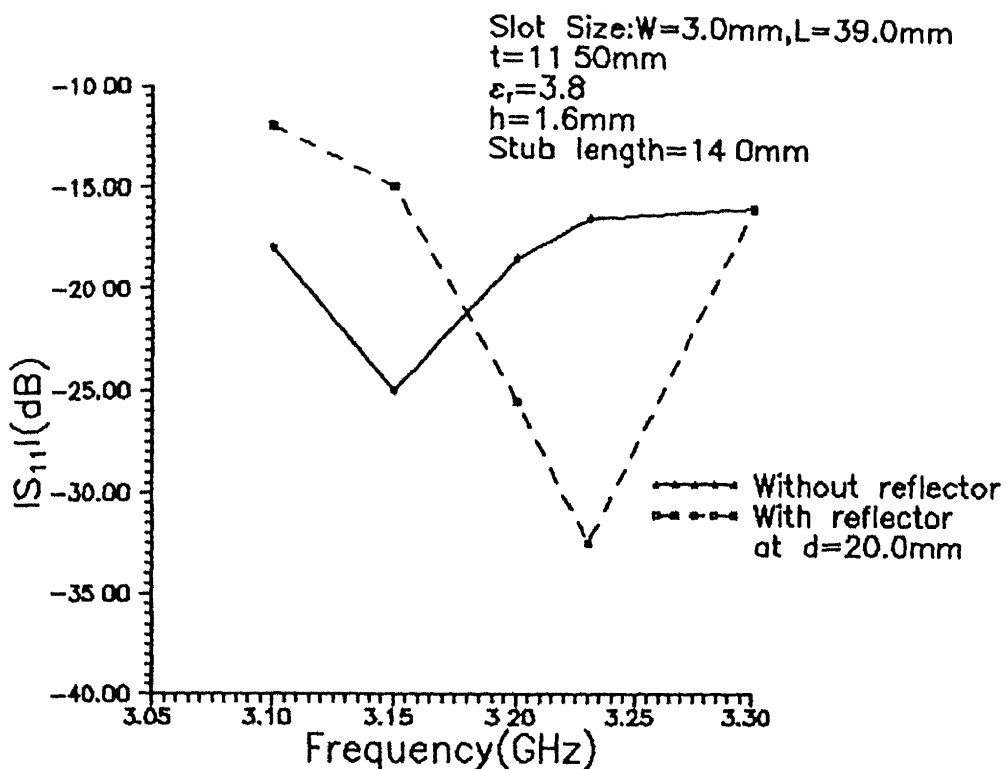


Fig 3 2 The magnitude of S_{11} versus frequency

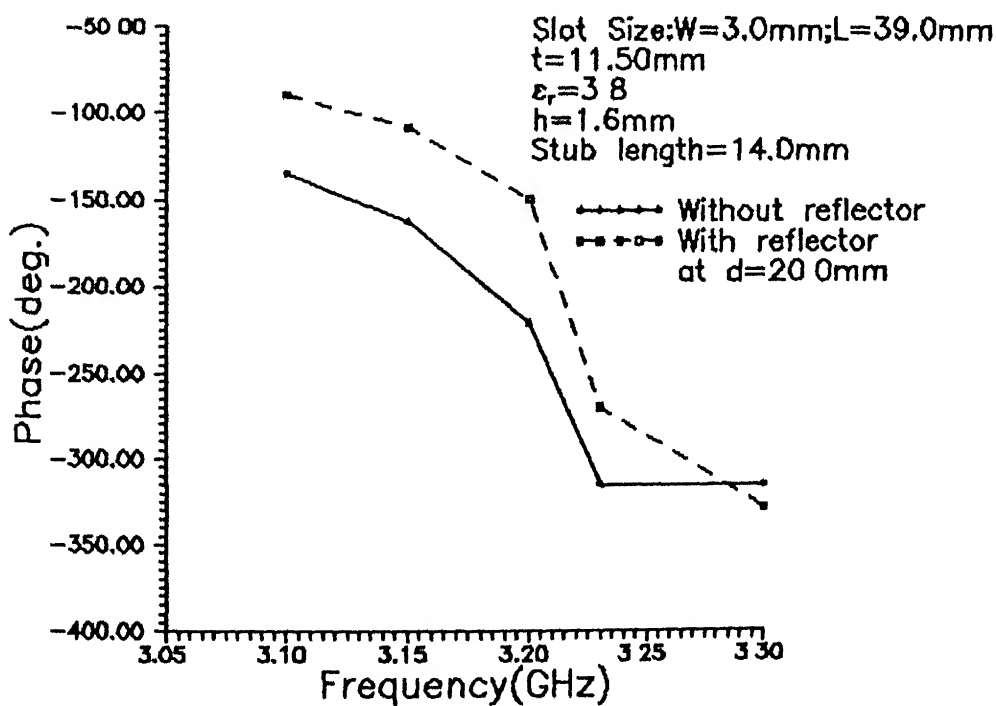


Fig. 3 3 : The phase of S_{11} versus frequency

observed that the reflection coefficient level is higher with the reflector.

The S_{12} magnitude and phase are measured as the transmission coefficient between the ports 1 & 2, making the third slot shorted with the ground plane and the element spacing is $0.7\lambda_0$. The Fig. 3.4 & 3.5 shows the variation of magnitude and phase of S_{12} with respect to frequency.

In the same way S_{13} is measured, as the transmission coefficient between ports 1 and 3, making second slot shorted with the ground plane and the element spacing is $1.4\lambda_0$. The Fig. 3.6 and 3.7 shows the variation of magnitude and phase versus frequency respectively. In both the cases it is observed that the coupling level is higher with the reflector.

The self and mutual admittances of slots at 3.2 GHz are evaluated by $[S]_{3x3}$ matrix in free space and with the reflector. The admittance matrices $[Y]_{3x3}$ are evaluated, in each case, using the following relation

$$Y = \sqrt{Y_0} (I-S) (I+S)^{-1} \sqrt{Y_0} \quad (3.1)$$

Here I is the $3x3$ unit matrix. Since the reference plane of $[S]$ matrices are at coax transition, hence to find the $[S]$ matrices of slots, the measured $[S]$ matrices are transformed to the slot plane, using the phase shift property of $[S]$ matrix.

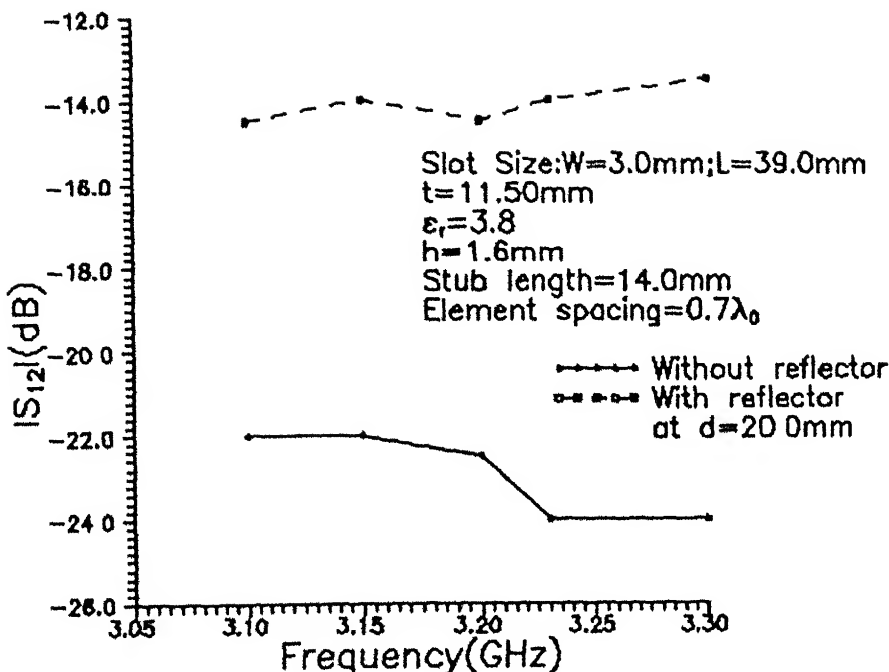


Fig. 3.4 . The magnitude of S_{12} versus frequency between two microstrip-fed slots

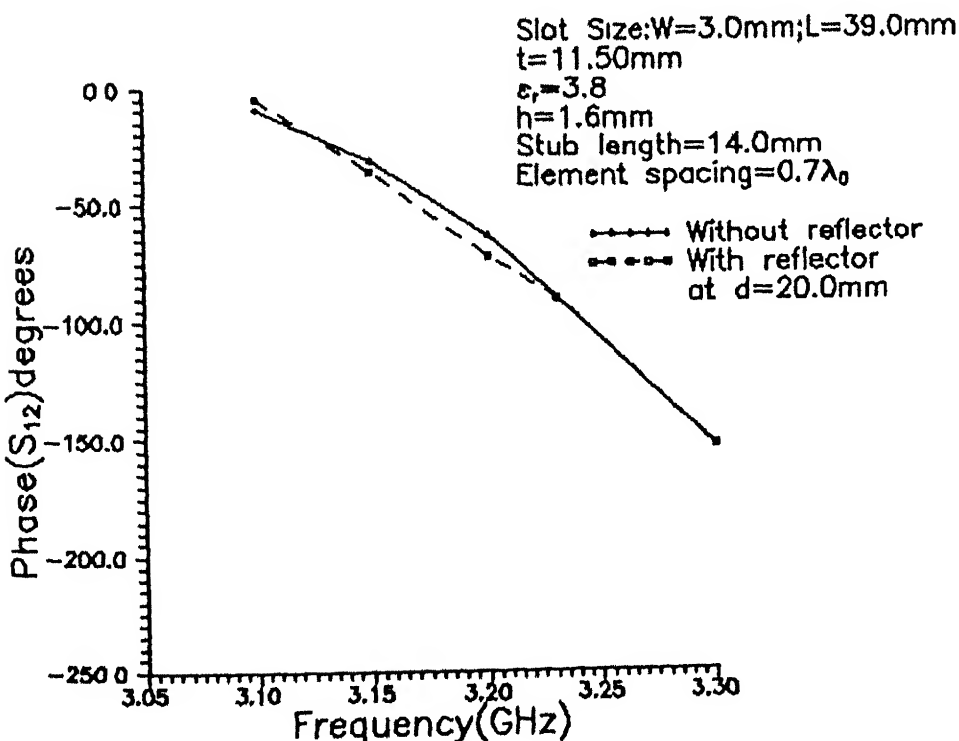


Fig. 3.5 . The phase of S_{12} versus frequency between two microstrip-fed slots

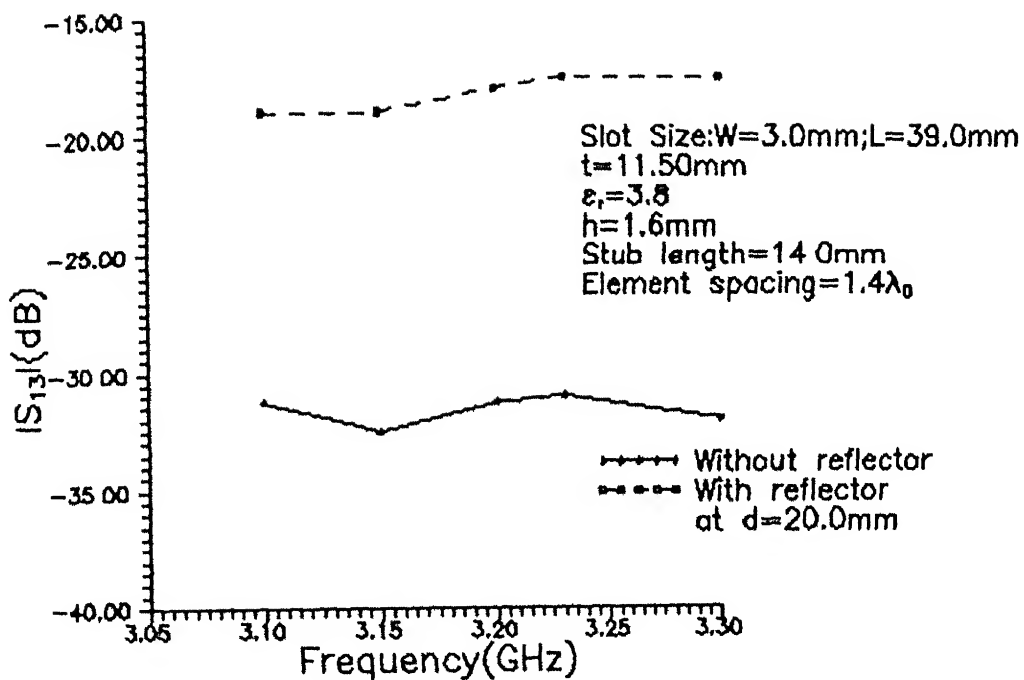


Fig 3 6 . The magnitude of S_{13} versus frequency between microstrip-fed slots

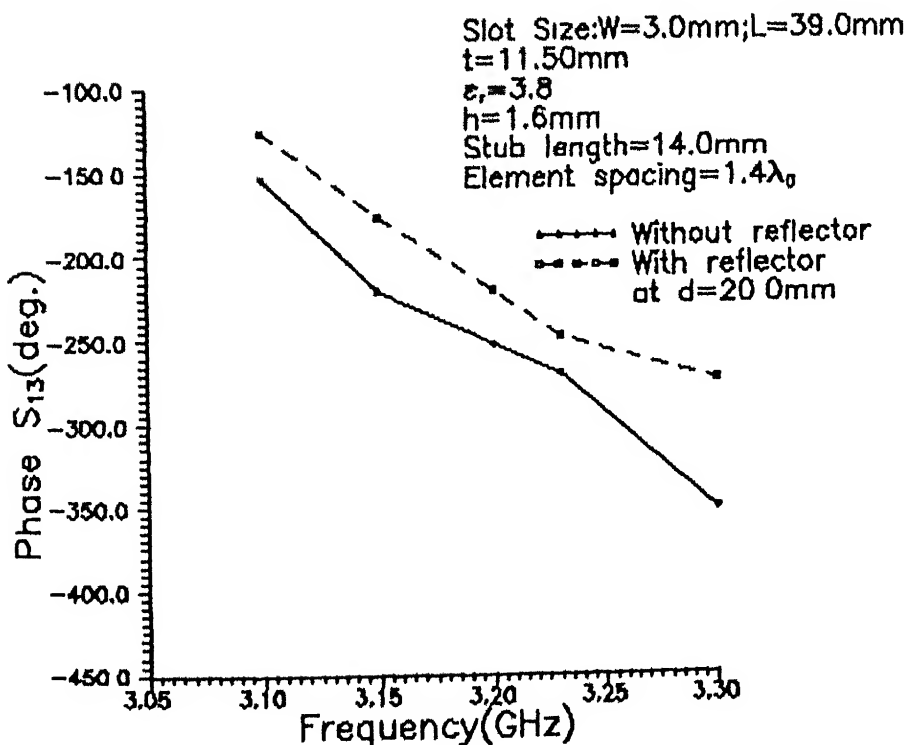


Fig. 3 7 : The phase of S_{13} versus frequency between

The Fig. 3.8 shows the magnitude variation of Y_{12} as element spacing and Fig. 3.9 shows the phase variation of Y_{12} versus element spacing with or without reflector

3.3 DIPOLE/SLOT FORMULATION

A center-fed rectangular slot in a large ground plane is complimentary to a center-fed strip dipole in free space, each of the same dimensions. The slot impedance and dipole impedance are related to each other by equation (2.1). The Booker's relation is one of the most important results in antenna theory. It extends the entire study on the self-impedance of center-fed slender dipoles to apply to a center-fed complementary slot in a large ground plane. The Booker's relation also applies to the ratio of the dipole mutual impedance to the slot mutual admittance [Page 344, (12)] in the generalized case of two or more elements

$$Z_{mn}^d / Y_{mn}^s = \eta^2 / 4 \quad (3.2)$$

This can be summarized by the equation

$$[Y^s] = \frac{4}{\eta^2} [Z^d] \quad (3.3)$$

Here $[Y^s]$ is the admittance matrix of the slot array and $[Z^d]$ is the impedance matrix of the complimentary dipole array and $\eta = 377 \Omega$ is the characteristic impedance of free space.

To study the measured free space offset-fed mutual admittance data of longitudinal slots, to the mutual impedance of center-fed dipoles of equivalent radius, $a/\lambda_0 = 0.008$ (slot width 3.0 mm), the

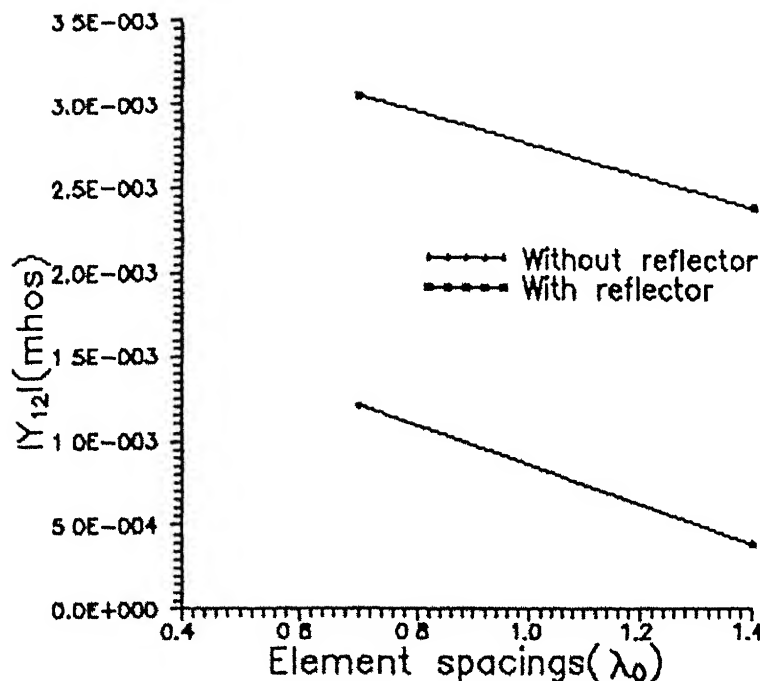


Fig 3.8 : The magnitude of measured mutual admittance of microstrip-fed slots as a function of spacing

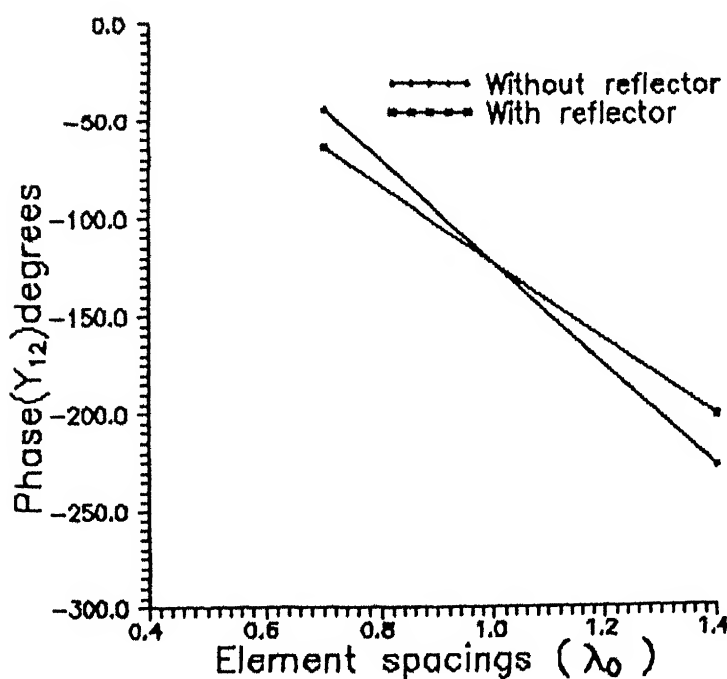


Fig. 3.9 : The phase variation of measured mutual admittance of microstrip-fed slots as a function of spacing

data of self-impedance (Z) and mutual impedance (Z_{12}) of center-fed dipoles (placed collinearly in free space) are evaluated using the following equations [Page 302, 326-333 (12)].

$$Z = \left[122.65 - 204 \ln kl + 110(kl)^2 \right] - j \left[120 \left(\ln \frac{2l}{a} - 1 \right) \cot kl - 162.5 + 140 \ln kl - 40(kl)^2 \right] \quad (3.4)$$

Here $1.3 \leq kl \leq 1.7$ and $0.001588 \leq a/\lambda_0 \leq 0.009525$, $2l$ is the dipole length and $k = 2\pi/\lambda_0$.

The real (R_{12}) and imaginary (X_{12}) components of mutual impedance between two collinear dipoles of equal lengths = $2l_1$, placed at a distance z (center to center) are evaluated using the equations (3.5) and (3.6).

$$R_{12} = \frac{30}{(\sin kl_1)^2} \int_{-l_1}^{l_1} \left(\frac{\sin kr_1}{r_1} + \frac{\sin kr_2}{r_2} - 2\cos kl_1 \frac{\sin kr}{r} \right) \sin k(l_1 - |x|) dx \quad (3.5)$$

and

$$X_{12} = \frac{30}{(\sin kl_1)^2} \int_{-l_1}^{l_1} \left(\frac{\cos kr_1}{r_1} + \frac{\cos kr_2}{r_2} - 2\cos kl_1 \frac{\cos kr}{r} \right) \sin k(l_1 - |x|) dx \quad (3.6)$$

$$\text{Here } r = (z + x) \quad (3.7)$$

$$r_1 = (z + x - l_1) \quad (3.8)$$

$$r_2 = (z + x + l_1) \quad (3.9)$$

and r , r_1 , r_2 , l_1 and x are normalized to λ_0 .

The $[Z^d]$ matrix of dipoles are evaluated for lengths 0.375, 0.50 and $0.625\lambda_o$, $a/\lambda_o = 0.008$, and $[Y^s]$ matrix of center-fed slots are obtained using (3.3). The center-fed $[Y^s]$ matrix is transformed to the offset-fed $[Y^s]$ matrix using $\cos^2\theta$ shape of Fig 2.4. The Fig 3.10 shows the variation of mutual admittance $|Y_{12}^s|$ of offset-fed slots of lengths 0.375, 0.500 and $0.625\lambda_o$ in free space, along with the magnitude of measured Y_{12} without reflector (Y_{12}^{mf}). The measured Y_{12}^{mf} of slots are very close to the complimentary slot length of $0.625\lambda_o$.

3.4 FINAL MUTUAL COUPLING MODEL

Fig 3.8 shows that the magnitude of mutual coupling between elements is higher with the reflector and Fig. 3.10 shows that the magnitude of mutual coupling between the slots without reflector is close to the complimentary slot length of $0.625\lambda_o$ in free space, however the little deviation may be attributed to the surface wave effect on the dielectrics and experimental error. As such no study of mutual coupling is available with the reflector, hence a model is evolved for the same. In this model it is presumed that the measured mutual coupling (Y_{12}^{mr}) between the slots, in the ground plane of a dielectric with a metallic sheet as reflector, is composed of two parts :

A part of the external coupling due to free space wave (Y_{12}^f) and

A part of the internal coupling due to the reflector (Y_{12}^r)
So

$$Y_{12}^{mr} = Y_{12}^f + Y_{12}^r \quad (3.10)$$

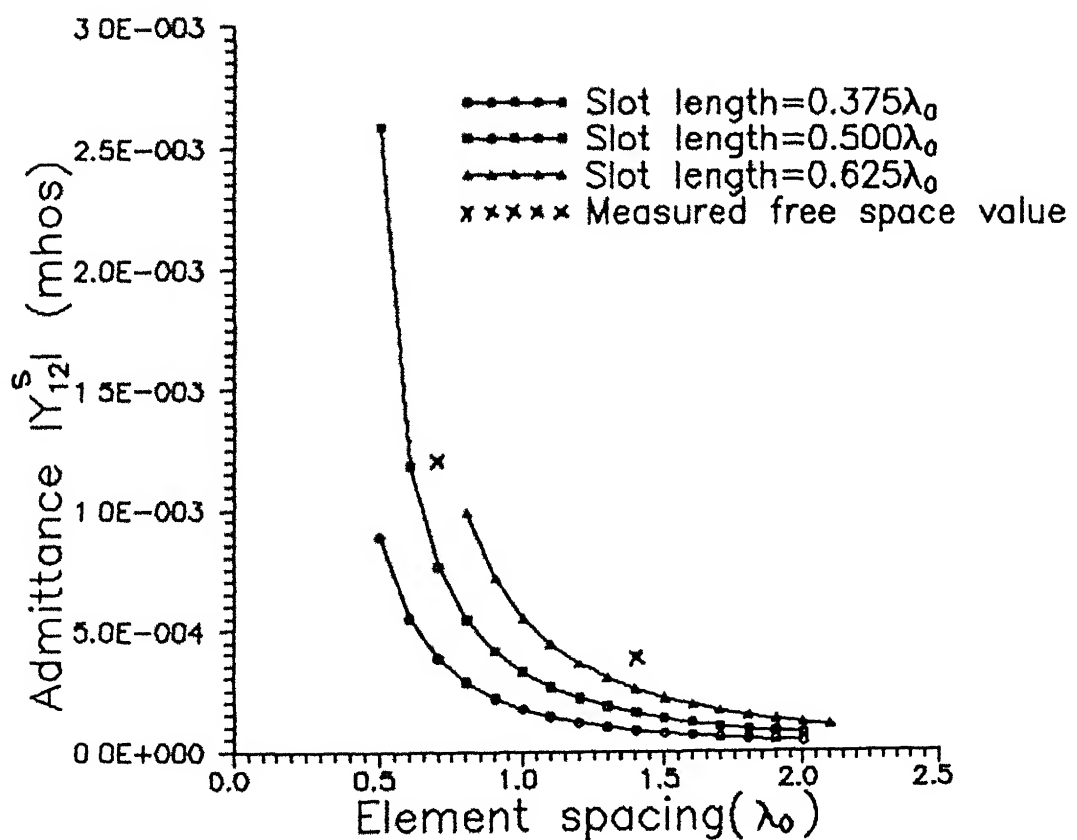


Fig 3.10 : The magnitude variation of mutual admittances of offset fed ($t = 0.123\lambda_0$) collinear complementary slots in free space, as a function of element spacing

The Y_{12}^f are evaluated using the half value of $0.625\lambda_0$ (complementary slot length) curve of Fig. 3.10.

The magnitude and phase at subsequent spacings are evaluated after fitting the curves on the half values as shown in Fig. 3.11 and 3.12. The equations for magnitude and phase are

$$\frac{Y_{12}^s}{2} = Y_{12}^f(\text{magnitude}) = 0.000279364 * X^{-(2.26598)} \quad (3.11)$$

and

$$Y_{12}^f(\text{phase}) = -375.972X + 222.654 \quad (3.12)$$

Here X is the element spacing (S/λ_0).

Similarly using the measured value of Y_{12}^{mr} (with the reflector) and Y_{12}^f , Y_{12}^r are evaluated using the equation (3.10). The values are $4.9792E-03/69.58^\circ$, $4.8616E-03/-197.92^\circ$ at element spacing of 0.7 and $1.4\lambda_0$ respectively. After curve fitting at Y_{12}^r values, the further data for magnitude and phase are evaluated using the equations (3.13) and (3.14) respectively.

$$Y_{12}^r(\text{magnitude}) = \text{Exp} [-0.00505856X] * 0.00499686 \quad (3.13)$$

$$Y_{12}^r(\text{phase}) = -183.343X + 58.76 \quad (3.14)$$

Here X is the element spacing (S/λ_0).

The magnitude and phase of Y_{12}^f and Y_{12}^r are shown in Fig. 3.13 and 3.14, respectively. The resultant mutual coupling, between the slots, $Y_{12}(x)$ are evaluated using the relation

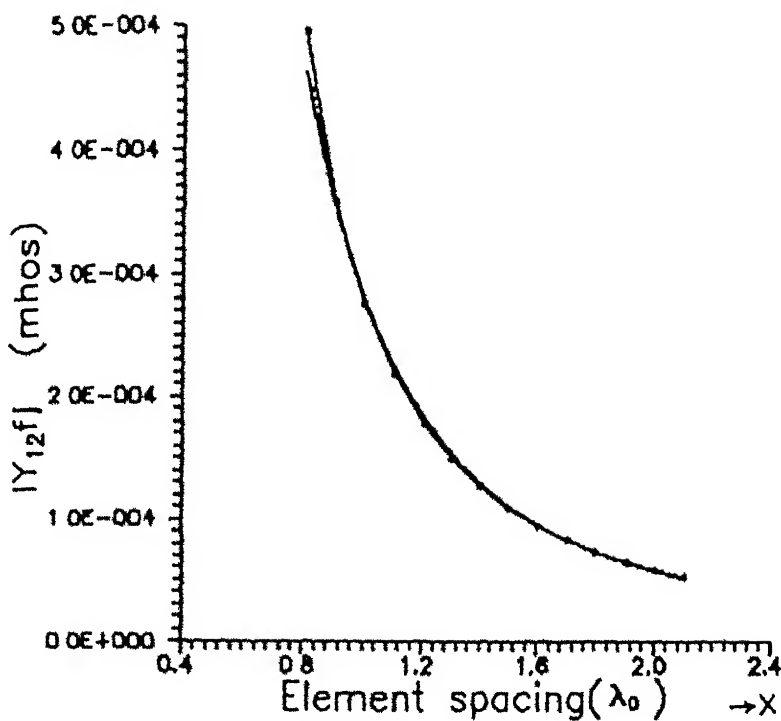
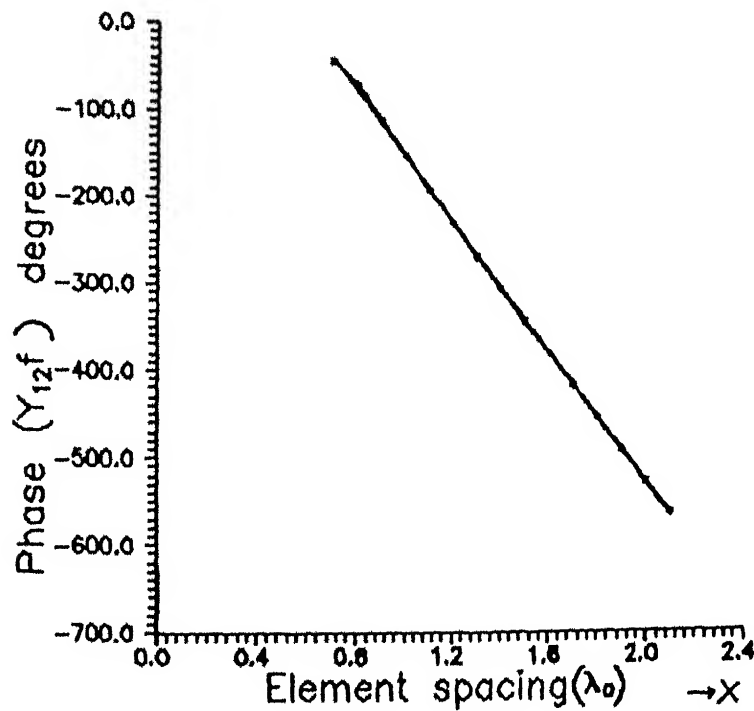


Fig 3.11 . Variation of mutual admittance (half of magnitude) versus spacing of a offset fed complementary slot ($L = 0.625\lambda_0$) in free space



----- Variation of mutual admittance vs.

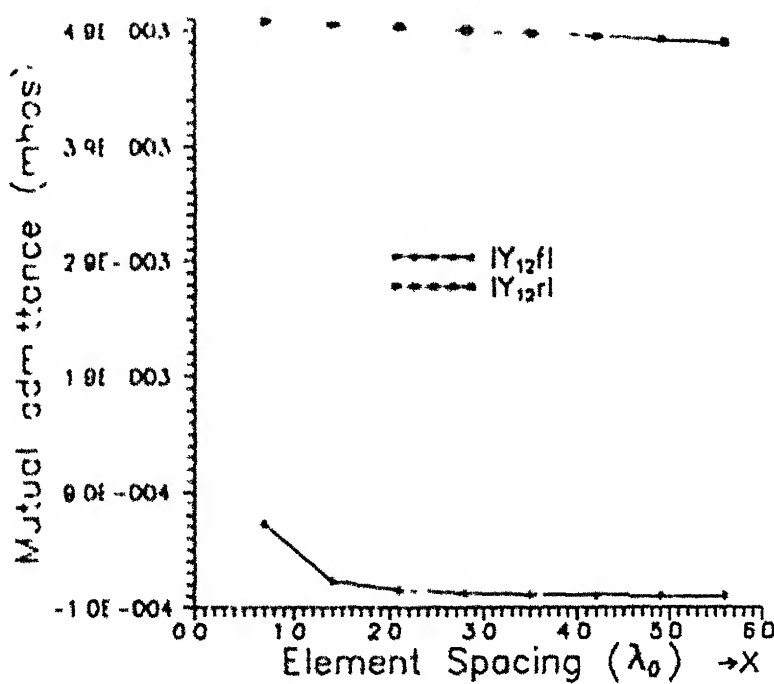
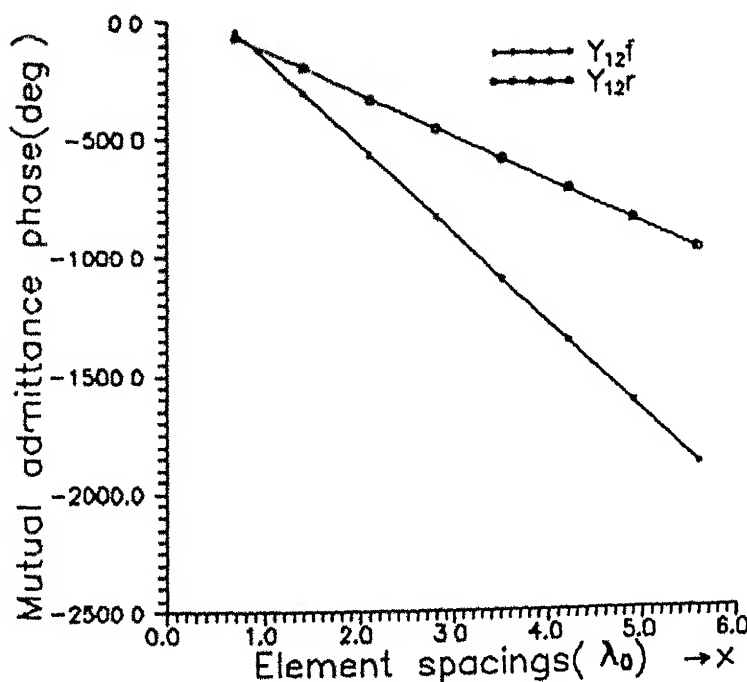


Fig 3.13 : Magnitude variation of mutual admittance as a function of spacing in free space and with reflector



$$Y_{12}(x) = Y_{12}^f(x) + Y_{12}^r(x) \quad (3.15)$$

and shown in Fig. 3.15 and 3.16

3.5 CONCLUSION

The mutual coupling measurements have been made for the slots at 3.2 GHz. It is observed that the coupling with the reflector is more than the free space. As the free space part of mutual coupling is compared with the complementary dipoles in free space, it can be inferred that without reflector, the coupling is in good approximation to the complementary dipoles. Hence the coupling with the reflector can be treated as composed of two parts, a part of the external coupling due to free space wave and a part of the internal coupling due to the reflector.

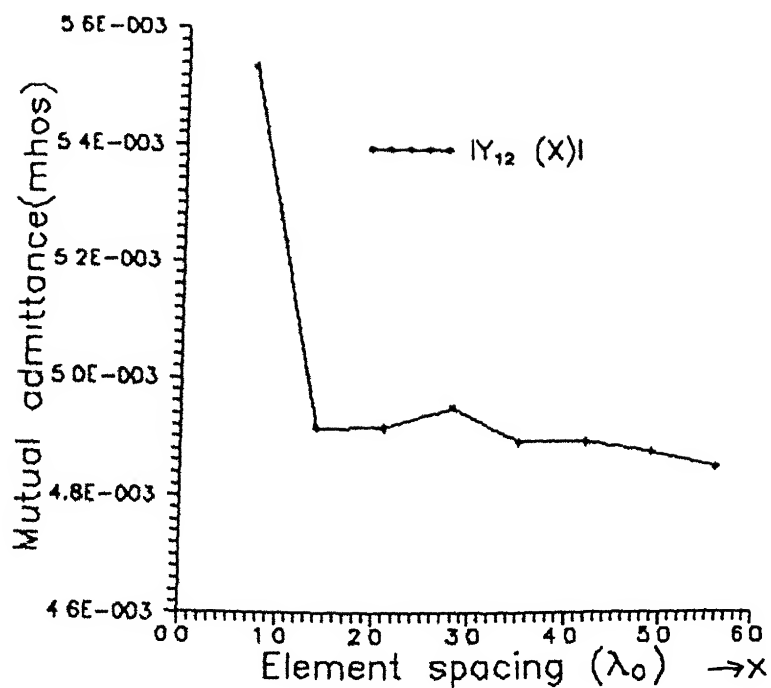
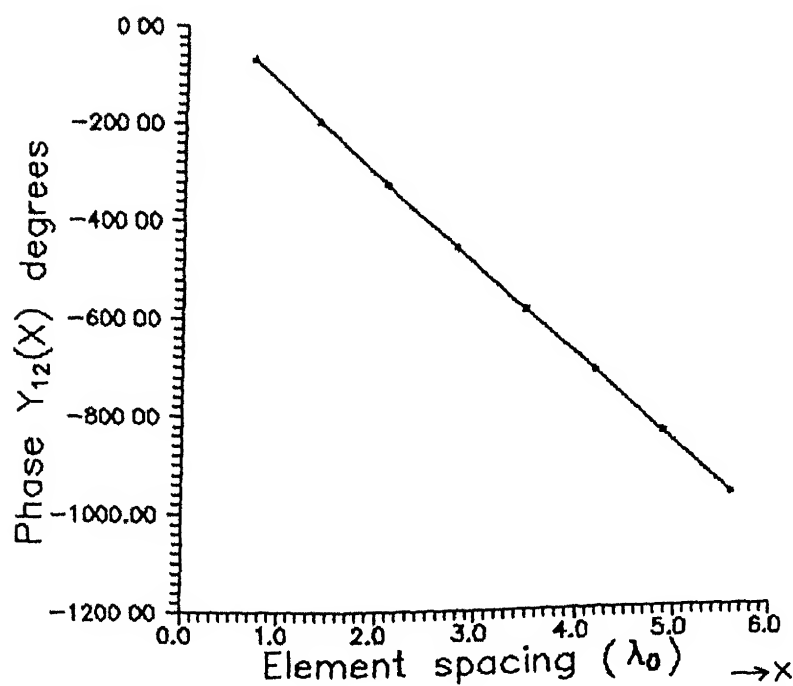


Fig 3 15 . Magnitude variation of mutual admittance as a function of spacing, of microstrip-fed slots with reflector



..... of mutual admittance as

CHAPTER 4

ARRAY DESIGN

4.1 ARRAY SPECIFICATION

It is decided to design a broadside linear array with the following specifications.

- . Operating frequency = 3.2 GHz
- . Band width = 10% (approx)
- . Side lobe level \approx 20 dB
- . Coverage = Omni in horizontal plane
- . Gain = 8 dB

4.2 ARRAY FACTOR DESIGN

To design an array as per specifications the Taylor distribution is taken and array factor is calculated using The Linear Antenna Array Analyzer (LAARAN) software [13]. The input data for LAARAN are $n = 3$, S.L.L. = 20 dB, No. of elements 8, element spacings $0.7\lambda_0$ and frequency = 3.2 GHz. The computed array factor is as follows

- . Directivity = 10.52 dB
- . Beam width = 10.17 (deg) and

the voltage excitation coefficients for slots are in Table 4.1, the phase of each element is zero.

S No	V_n	Voltage Coefficient
1	V_1	0 539
2	V_2	0 672
3	V_3	0 863
4	V_4	1 000
5	V_5	1 000
6	V_6	0 863
7	V_7	0 672
8	V_8	0 539

4.3 DESIGN COEFFICIENTS

The element for the design of array has been fully characterized and discussed in chapter 2. Hence the microstrip-fed slot of $W=3.0$ mm, $L=39.0$ mm and $t=1.5$ mm is chosen as an element for the array. The element spacing is $0.7\lambda_0$ and eight elements are taken for the array design.

4.4 ACTIVE IMPEDANCE COMPUTATION FOR THE ARRAY

The mutual coupling among the elements affects their self-admittances, hence the active admittances of slots are different from the self-admittances of each slot. The active admittance Y_m^a of the m^{th} slot can be computed using the equation (4.1) (Page 401- [12])

$$Y_m^a = \sum_{n=1} \left(\frac{n}{V_m} \right) Y_{mn} \quad (4.1)$$

Here, Y_{mm} is the self-admittance of the m^{th} slot and Y_{mn} is the mutual admittance between the m^{th} and n^{th} slots. Thus the active admittance is the sum of self-admittance and the voltage-weighted sum of the mutual admittances.

The magnitude and phase of mutual admittances of all the eight slots are computed from the Fig. 3.15 and 3.16. Using these values and the corresponding voltage excitation coefficient (Table 4.1), the active admittance of each slot is computed by equation (4.1). The active impedances $Z_i^a = 1/Y_i^a$ of slots are given in Table 4.2.

Table 4.2 : Active Impedances of Slots

S No.	Z_m^a	Active Impedance (Ohms)
1	Z_1^a	$82.17 + j32.14$
2	Z_2^a	$69.74 + j27.28$
3	Z_3^a	$84.91 + j40.74$
4	Z_4^a	$74.53 + j30.19$
5	Z_5^a	$74.53 + j30.19$
6	Z_6^a	$84.91 + j40.74$
7	Z_7^a	$69.74 + j27.28$
8	Z_8^a	$82.17 + j32.14$

4.5 MATCHING/FEED NETWORK DESIGN

To design the feed network, the power levels for each slot are computed based on the resistive part of active impedance (Table 4 2) and the corresponding voltage excitation coefficients (Table 4 1) The reactive part of the slots are cancelled out by the open-circuited microstrip line (characteristic impedance 100Ω) stubs The length of stubs are 11.44, 11.85, 10.75 and 11.6 mm. A simple symmetrical power divider network is designed for the slots As an example the feed network for first two slots is designed as follows. The real part active impedance of the first slot is 82.17Ω and of the second is 69.74Ω These impedances are transformed to 70Ω using quarter wave microstrip line transformer of impedances 75.84 and 70 ohms respectively. The transformed 70Ω lines of these two slots are joined to another 70Ω line as a T-junction as shown in Fig 4 1.

Depending on power level distribution for first slot $P_1 = 3.542$ milliwatt and second slot $P_2 = 6.4698$ milliwatt, the value of quarter wave transformers t_1 , t_2 and t_3 are calculated based on R_1 , R_2 and R_{in} values at T-junction Since $P_1/P_2 = R_2/R_1 = 0.547$ and the power level at first slot is less than the second, a compensation in R_{in} is provided i.e. $R_{in} = 70/\sqrt{2.8}$, since $(P_1+P_2)/P_1 = 2.8$. Now as $R_{in} = (R_1+R_2)/R_1 R_2$, hence $R_1 = 118.7 \Omega$ and $R_2 \approx 65 \Omega$ is calculated. The corresponding t_1 , t_2 and t_3 with respect to 70Ω line is 91.16, 67.45 and 54.22 ohms respectively The computations for other slots are also performed in the same manner and the overall feed network (with matching sections

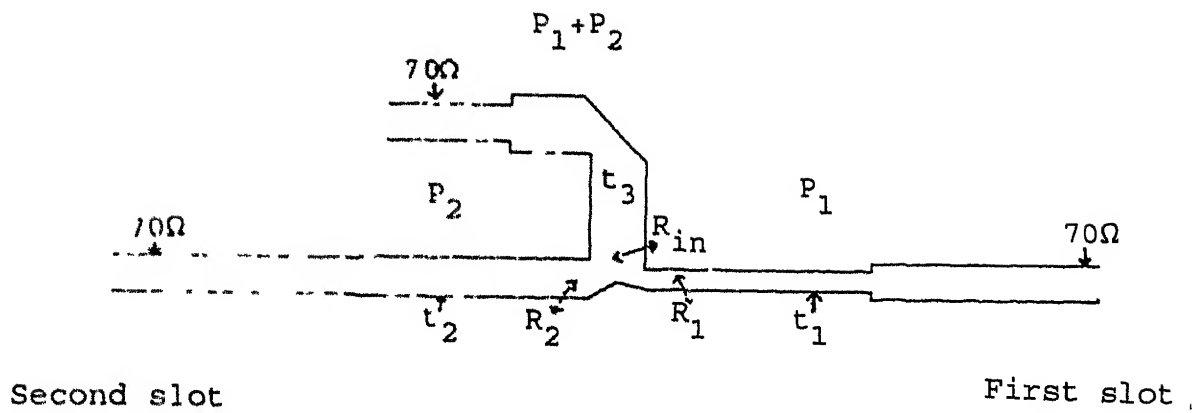


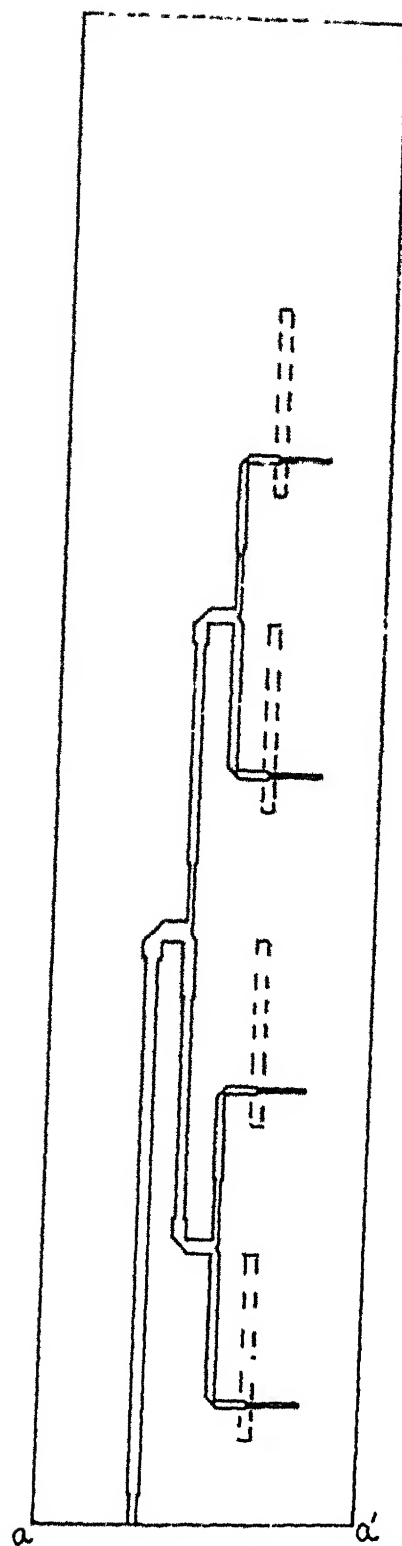
Fig. 4.1 : Design of feed network for First and Second slot

included) is shown in Fig 4.2 and 4.3 The bending of microstrip lines are 'Optimal Right-Angle Metered Bend' (5.5,2 Page 289-90 [14]) and for T-junctions are 'Optimal Microstrip Line T' (5.5,12 2 Page 315 [14])

4.6 FABRICATION AND TESTING

The array is fabricated on a glass epoxy substrate by conventional photo-etching technique. The feeding network along with slots as per specifications is initially designed for the whole array. Now as the length of the array is 63 cm (approx.), it was not possible to etch the array on a substrate in a single piece. Hence, the initial design is cut into two pieces and then each piece of array is fabricated by photo-etching technique on glass epoxy substrate ($\epsilon_r = 3.8$, $h = 1.6$ mm). Later on these pieces are joined. The 'aa'', of part 'A' (Fig. 4.2) is joined to 'aa'', of part 'B' (Fig. 4.3) to make an array. The ground plane is joined by a copper tape and the feeding line is firmly joined by soldering. The 50Ω line of matching network is transformed to a 50Ω coax transition. The complete array is placed on a reflector at $d = 20.0$ mm by spacers. The size of array is 6 cm x 63 cm. To confine the radiations in 120° area, the sides of the reflector is tapered at 120° , as shown in Fig 4.4

The S_{11} measurements of the array is performed on a HP-8410 Network Analyzer in the frequency range of 2.7 to 3.8 GHz. To measure the gain and radiation pattern of the array, two dipoles resonant at 3.2 GHz are fabricated. The return loss of these dipoles are less than 10 dB in the frequency range of 3.0-3.3 GHz.



4.2 Configuration of microstrip-fed slot array. Part 'A'

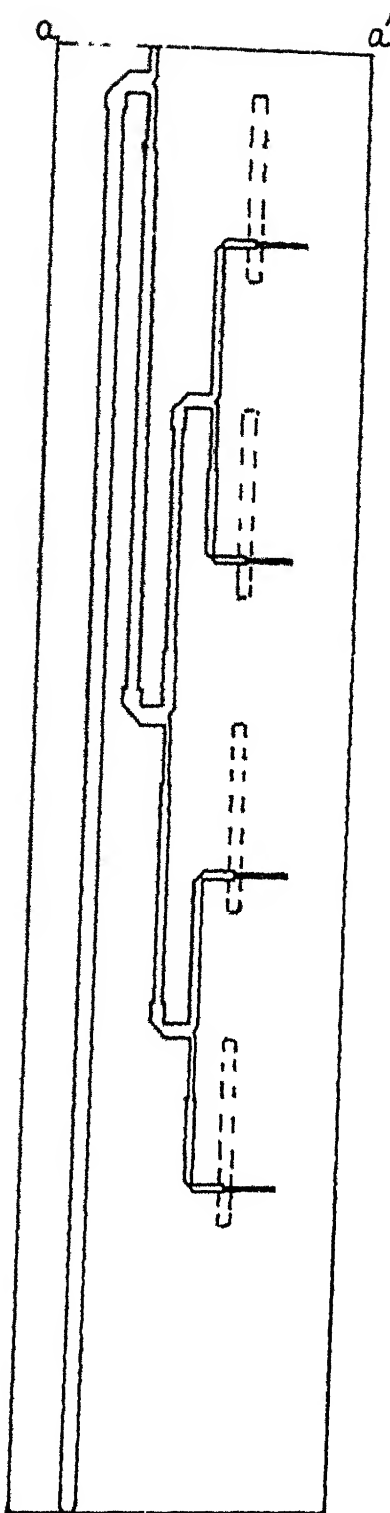


Fig. 4.3 . Configuration of microstrip-fed slot array. ~~Part 10~~

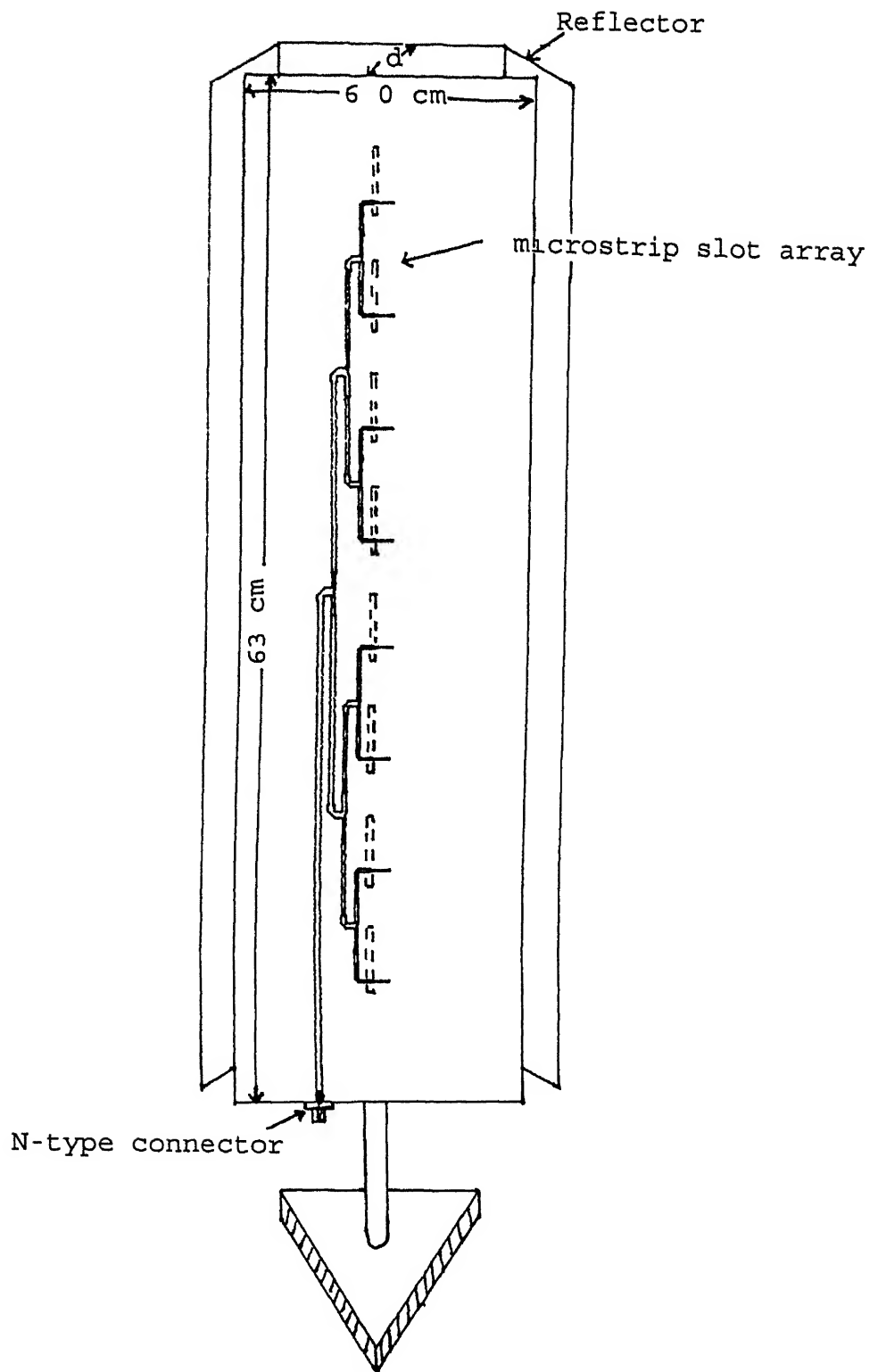


Fig. 4 4 . Configuration of eight-element micro-strip-fed slot array

The radiation pattern are measured making the array as receiving antenna and the dipole as a transmitting antenna at 3.2 GHz. The E-plane measurements are made making array vertical and H-plane measurements are made making it horizontal. The dipole orientation is also made according to the plane of measurement. The array is rotated from 0° to 360° in steps and the received power is measured on a VSWR meter.

The gain of the array is measured by three antenna method at 3.2 GHz. In this method one antenna (D_1) is used as a transmitting antenna and the power received by the second antenna (D_2), $P_{r_{D2}}$ is measured. In the next step, the second antenna is replaced by the array and the received power $P_{r_{array}}$ is measured. In the third case, the second antenna is used as a transmitting antenna and the array is used as a receiving antenna. The power received by array, $P_{r_{array}}$ is measured. Now solving the following three simultaneous equations of Frii's transmission formula, gain of each antenna is calculated

$$G_{D1} + G_{D2} = 20 \log_{10} \left(\frac{4\pi R}{\lambda} \right) - 10 \log_{10} \frac{P_A}{P_{r_{D2}}} \quad (4.2)$$

$$G_{D1} + G_{array} = 20 \log_{10} \left(\frac{4\pi R}{\lambda} \right) - 10 \log_{10} \frac{P_A}{P_{r_{array}}} \quad (4.3)$$

$$G_{D2} + G_{array} = 20 \log_{10} \left(\frac{4\pi R}{\lambda} \right) - 10 \log_{10} \frac{P_A}{P_{r_{array}}} \quad (4.4)$$

Here G_{D1} , G_{D2} and G_{array} are the gain of the first dipole, second dipole and array respectively. P_A is the power available (transmitted), R is the distance between antennas and λ is the

wavelength of radiation. In the same way, the gain of antenna element is also computed

4.7 RESULTS

The Fig 4.5 shows the variation of $|S_{11}|$ with respect to frequency. It is observed that at 3.14 GHz, the VSWR is less than 1.8. However, in the frequency range of 3.1 to 3.3 GHz, the VSWR is less than 3.0. The Fig 4.6 and 4.7 shows, the pattern and excitation level distribution of array computed by LAARAN [13]. The Fig. 4.8 and 4.9 shows the measured E-plane and H-plane radiation pattern of the array. The E-plane beam width (3 dB down) is 100° and H-plane beam width (3 dB down) is 13° . The directivity of the array is evaluated using equation (4.5) (Page 25, [4]).

$$\text{Directivity} = \frac{41,253}{\theta_1^\circ \phi_1^\circ} \quad (4.5)$$

Here, θ_1° and ϕ_1° are the half-power beam widths in degrees.

The directivity of the array is 15.01 dB. The side lobes are around 10 to 12 dB down. The gain of the first dipole, G_{D1} , is 7.2 dB, the gain of the second dipole, G_{D2} , is 7.90 dB and the gain of the array, G_{array} , is 7.2 dB. The gain of the element is 1.82 dB. The array efficiency is 20%.

4.8 CONCLUSION

The gain of the resonant slot antenna is to be around 5 dB. However, the measured gain of the element is 1.82 dB. It is

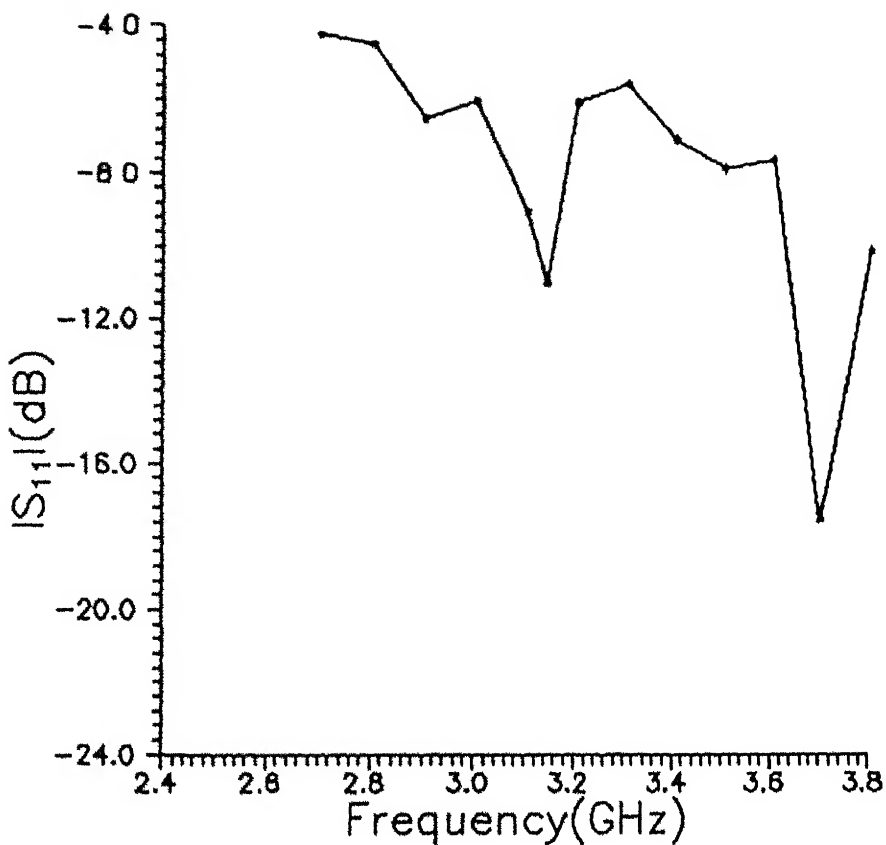


Fig 4.5 . Magnitude of S_{11} versus frequency of microstrip-fed slot array

Theoretical pattern of the Array

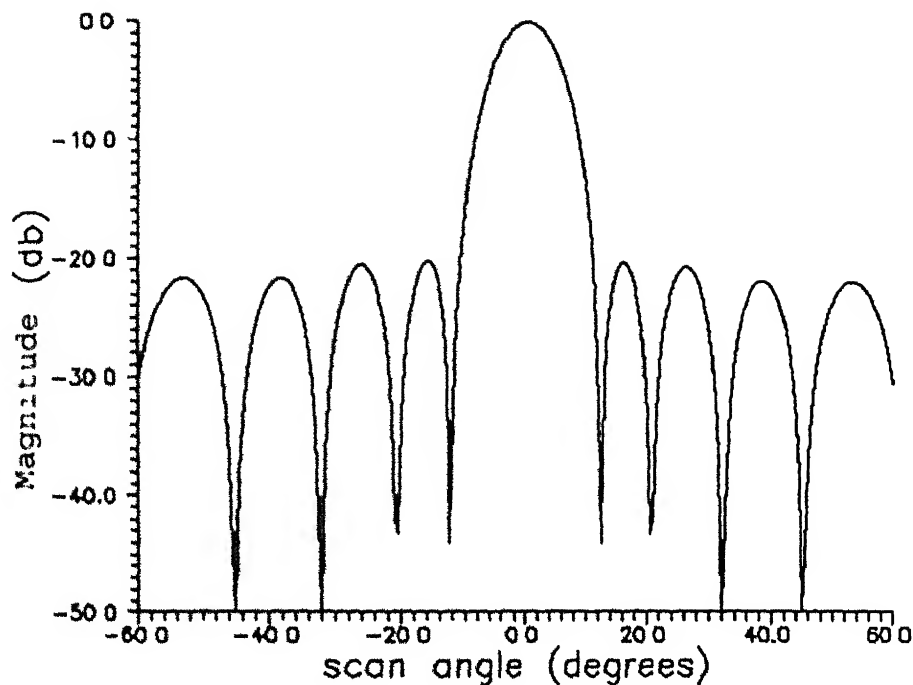


Fig. 4.6 : Theoretical pattern of the array computed by LAARAN [13]

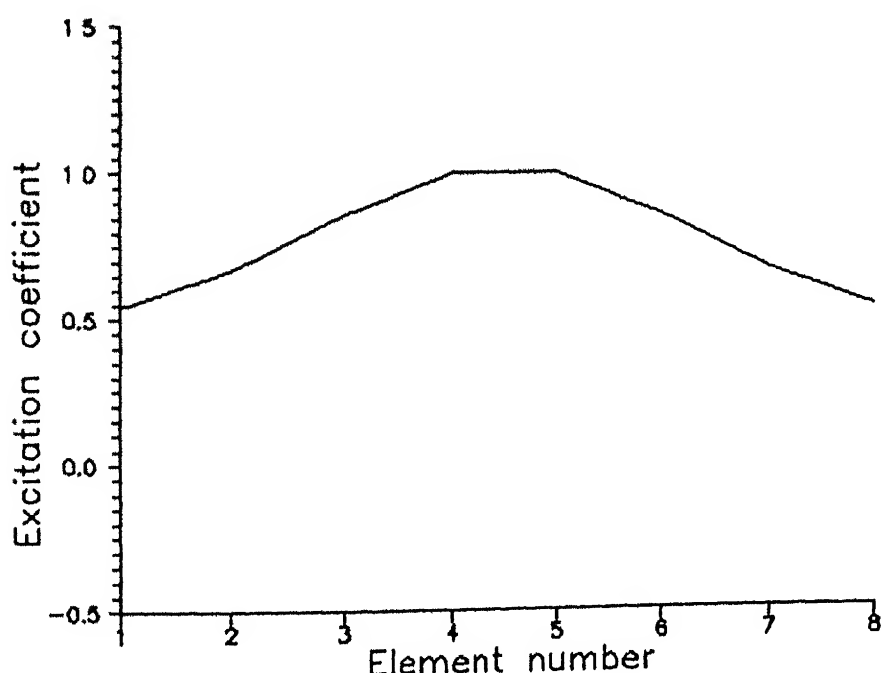


Fig. 4.7 : Excitation coefficient distribution of array vs element number computer by LAARAN [13]

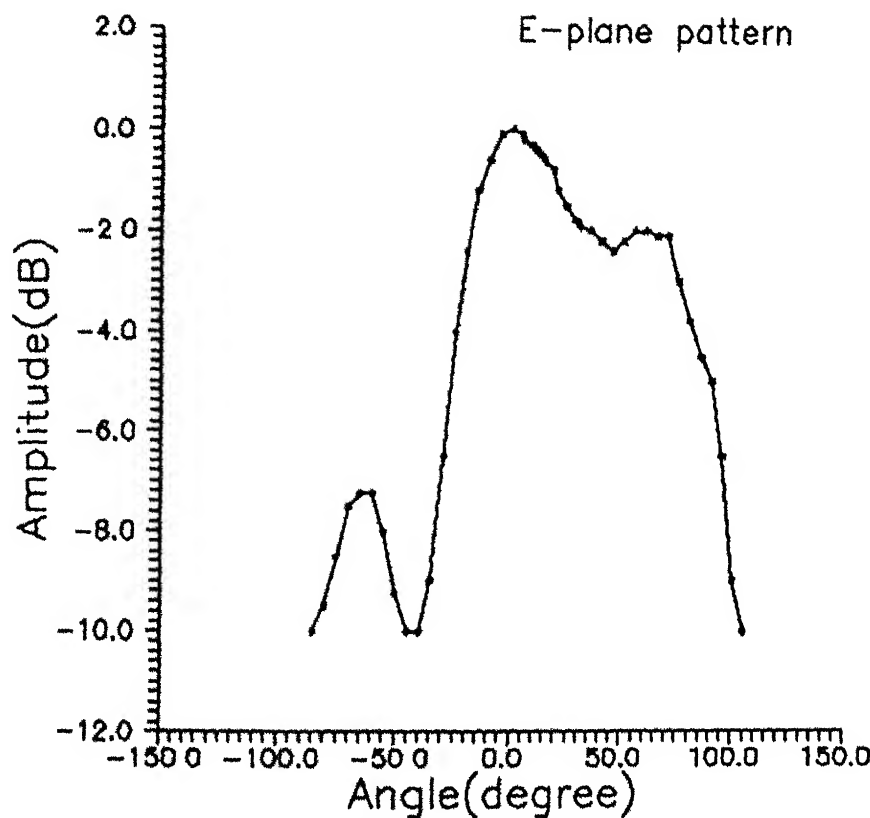


Fig. 4 8 · E-plane radiation pattern of microstrip-fed slot array of eight elements

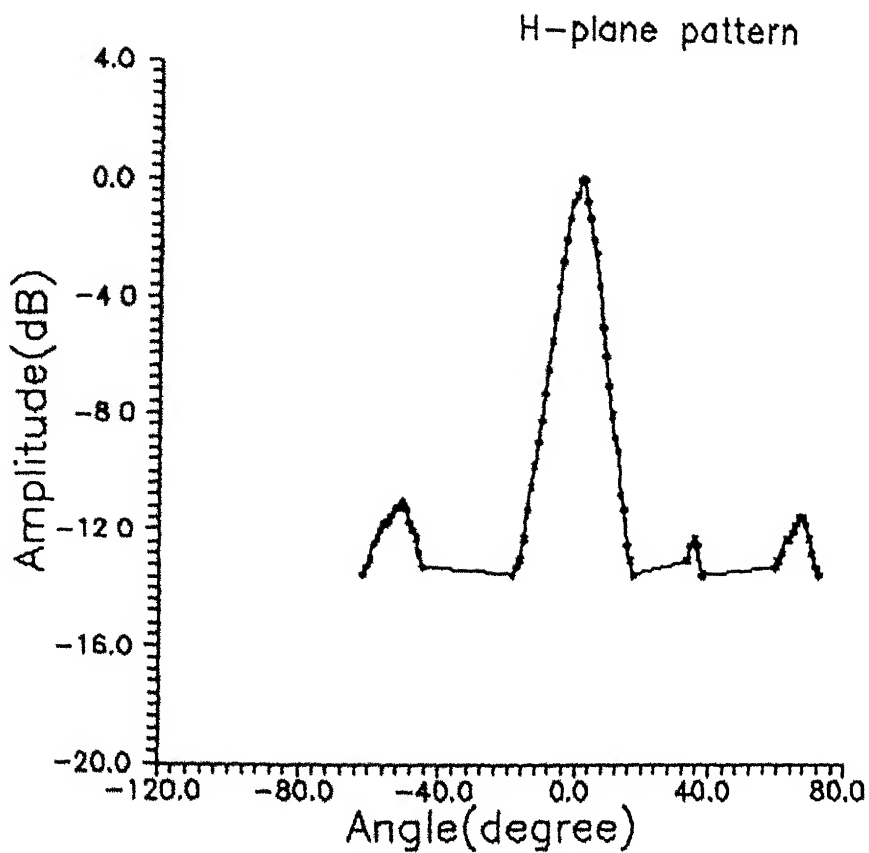


Fig. 4.9 . H-plane radiation pattern of microstrip-fed slot array of eight elements

approximately 3.2 dB less. This loss is mainly due to the dielectric loss. Similarly, the gain of the array is found 7.2 dB, which is also less than the expected value (8 dB). The reason for this may be attributed to the mainly dielectric loss, as glass epoxy is a lossy substrate and of feed line losses. The radiation pattern measurements are performed in the non-anechoic environment hence the increased side lobe level may be due to the reflection of walls etc. However, it can be concluded that the array can be used at frequency 3.2 GHz and the horizontal coverage of 100° (at 3 dB down) and 120° (at 5 dB down) can be obtained. The 9% bandwidth is at VSWR less than 3.0.

CONCLUSIONS

5.1 SUMMARY AND CONCLUSIONS

An omnidirectional coverage antenna of 3.2 GHz with high gain is required as a base station antenna for rural communication network. The omnidirectional coverage can be achieved by using three arrays, of 120° coverage, around a circle. In the present work, such a type of linear array is experimentally fabricated and tested. Before developing the array, an element of the array was characterized.

Initially, an offset-fed microstrip slot antenna, as an element of the array, was fabricated on a glass epoxy substrate. Models with different slot lengths and various feed points were printed. The input impedance of each was measured with various slot-to-reflector spacing. Based on these measurements, a resonant slot length of 39.0 mm, with offset feed point of 11.5 mm and reflector spacing of 20.0 mm was selected to be the element dimension for the final array. The input impedance, VSWR and radiation pattern of this antenna is evaluated experimentally. It is observed that the slot is resonant at frequency 3.23 GHz and the VSWR is less than 1.31 in the frequency range of 3.0-3.3 GHz. The radiation pattern of the element is having significant side lobes. The reason for this may be that the scattered radiations from the open sides between the slot and reflector is causing

interferences. This interference can be checked by proper bending of the sides of the reflector. A detailed study of this interference is required for the proper characterization of the element.

The mutual coupling among the slots is evaluated by fabricating three slots with proper feeding network on a glass epoxy substrate. The [S] matrices of offset-fed slots are measured with and without reflector and converted to [Y] matrices to obtain the mutual admittances of slots. The mutual coupling between slots consists of two parts, one external coupling due to free space wave and the other internal coupling due to the parallel plate guide modes excited between the ground plane and the reflector plate. The formulation for the mutual coupling of two slots in an infinite ground plane is available in the literature. This can be computed using dipole formulation and using Booker's relationship, one half of this taken as the external mutual coupling. There is no formulation available for internal mutual coupling therefore this was obtained via measurements. From the measured total mutual coupling the estimated external mutual coupled portion is subtracted to get the internal coupling alone. A detailed analysis of mutual coupling among the slots, with the reflector is required.

From the measured data of single slot and mutual coupling of slots, the linear array is fabricated on a glass epoxy substrate. The excitation coefficient for the calculation of active impedances of slots are evaluated using 'LAARAN'. The corporate

feed network is designed depending upon the power distribution among the slots of array. To achieve 120° coverage the sides of the reflector is tapered at 120° . The array was tested in the laboratory for input VSWR, gain and the pattern. The input minimum return loss at the center frequency is -11.0 dB and -7.0 dB (approx.) in the band 3.1 to 3.3 GHz. The measured array directivity is about 15 dB at 3.2 GHz and 120° , 5 dB beamwidth in the horizontal plane and 3 dB beamwidth is about 100° . The 120° coverage with less than 3 dB beamwidth can be obtained by adjusting the size of the substrate as well as of the reflector with proper tapering. The gain of the array is measured by three antenna method using Frii's transmission formula. The measured gain is 7.2 dB, which is less than the expected 8 dB including the loss. This loss in gain is attributed to lossy glass epoxy substrate. This can be overcome using a low loss microwave substrate like PTFE, RT duroid 5880.

5.2 SCOPE FOR FURTHER WORK

The design of array can be improved by considering the following points.

- (i) The array is to be fabricated on a low loss microwave substrate, like PTFE, RT duroid 5880.
- (ii) The mutual coupling with the reflector requires a detailed analytical study.
- (iii) As the reflector is placed parallel to the slot, the radiations from the boundaries requires a special study on it's effect on the radiation pattern.

(iv) The fabricated array covers a sector of 120° in the horizontal plane. An antenna could be fabricated by arranging three such arrays around a circle as shown in Fig. 1.5 to obtain omnidirectional coverage.

- [1] J.R. James and P.S. Hall, "Handbook of Microstrip Antennas", Vol. 2, Peter Peregrinus Ltd., London (U.K.), 1989.
- [2] J. Hirokawa, J. Wettergren, P. Kildal, M. Ando and N. Goto, "Calculation of External Aperture Admittance and Radiation Pattern of a Narrow Slot Cut Across an Edge of a Sectoral Cylinder in terms of a Spectrum of Two-Dimensional Solutions", IEEE Transactions on Antennas and Propagation, Vol. 42, No 9, pp 1243-1248, September 1994.
- [3] Y.T. Lo and S.W. Lee, Chapter 13, Page 33, "Antenna Handbook: Theory, Application and Design", Van Nostrand Reinhold Company, New York, 1988.
- [4] J.D. Kraus, Antennas, McGraw-Hill, 1950.
- [5] R. Janaswamy and D.H. Schaubert, "Characteristic Impedance of a Wide Slotline on Low-Permittivity Substrates", IEEE Trans on Microwave Theory and Techniques, Vol. MTT-34, No 8, pp 900-902, August 1986.
- [6] D.M. Pozar, "A Reciprocity Method of Analysis for Printed Slot and Slot-Coupled Microstrip Antennas", IEEE Transactions on Antennas and Propagation, Vol.AP-34, No.12, pp 1439-1446, December 1986.
- [7] B.N. Das and K.K. Joshi, "Impedance of a Radiating Slot in the Ground Plane of a Microstripline", IEEE Transactions on Antennas and Propagation, Vol. AP-30, No. 5, pp 922-926, September 1982.

- [8] D.N. Poddar, N.K. Jain, B.N. Das and K.K. Joshi, "Comments on Impedance of a Pulsating Slot in the Ground Plane of a Microstrip Line", IEEE Transactions on Antennas and Propagation, Vol. AP-34, No 7, pp 958-959, July 1986.
- [9] P.V. Rao, B.R., "Analysis of Cavity Backed Microstrip Slot Antenna", M.Tech. Thesis, Deptt. of Electrical Engineering, I.I.T. Kanpur, April 1995.
- [10] A. Axelrod, M. Kisliuk and J. Maoz, "Microwave Journal", pp 81-94, June 1989.
- [11] Y. Yoshimura, "A Microstripline Slot Antenna", IEEE Trans on Microwave Theory and Techniques, Vol. MTT-20, pp 760-762, November 1972.
- [12] R.S. Elliot, "Antenna Theory and Design", Prentice Hall, Inc Englewood Cliffs, New Jersey, 1981.
- [13] The Linear Antenna Array Analyzer (LAARAN), Artech House Inc., 1990.
- [14] B.C. Wadell, "Transmission Line Design Handbook", Artech House, 1991.

A

121273

EE-1996-M-FAL-MIC